Pathology International

Pathology International 2013; **63**: 45–55 doi:10.1111/pin.12028

Original Article

Unique mutation, accelerated mTOR signaling and angiogenesis in the pulmonary cysts of Birt-Hogg-Dubé syndrome

Teppei Nishii,[1] Mikiko Tanabe,[2] Reiko Tanaka,[4] Tetsuhiro Matsuzawa,[4] Koji Okudela,[3] Akinori Nozawa,[2] Yukio Nakatani[5] and Mitsuko Furuya[3]

[1]Respiratory Disease Center, and [2]Diagnostic Pathology, Yokohama City University Medical Center, [3]Department of Pathology, Yokohama City University Graduate School of Medicine, Yokohama, [4]Medical Mycology Research Center, Chiba University and [5]Department of Diagnostic Pathology, Chiba University Graduate School of Medicine, Chiba, Japan

Birt-Hogg-Dubé syndrome (BHD) is an autosomal dominant disorder characterized by fibrofolliculomas, renal tumors and pulmonary cysts with repeated pneumothorax. This disorder is caused by mutations in the gene that encodes folliculin (FLCN). FLCN is known to be involved in the signaling of mammalian target of rapamycin (mTOR). We investigated the lung of a BHD patient who presented with a unique mutation. A 33-year-old woman visited our hospital due to repeated pneumothorax. Histopathologic study of the resected lung demonstrated multiple epithelial cysts. An increase of blood vessels was observed in the vicinity of subpleural cysts. Genomic DNA analysis revealed heterozygous mutation at the 3′ end of intron 5 of the *FLCN* gene. Total mRNA and protein were extracted from the resected lung tissue. RT-PCR and sequence analysis demonstrated the production of exon 6-skipped *FLCN* mRNA. In Western blotting, the band intensities of phospho-mTOR, phospho-S6, phospho-Akt, hypoxia-inducible factor (HIF)-1α and vascular endothelial growth factor (VEGF) were increased in the BHD lung compared with normal lungs. Histopathologic analysis demonstrated strong immunostainings of mTOR signaling molecules in cyst-lining cells. Collective data indicates that dysregulation of mTOR signaling facilitates S6-mediated protein synthesis and HIF-1α-mediated angiogenesis, which may contribute to the development of pulmonary cysts in this disorder.

Key words: angiogenesis, Birt-Hogg-Dubé syndrome, exon-skipping, mTOR signaling, pneumothorax, pulmonary cysts

Correspondence: Mitsuko Furuya, MD, PhD, Department of Molecular Pathology, Yokohama City University Graduate School of Medicine, 3-9 Fukuura, Kanazawa-ku, Yokohama 236-0004, Japan. Email: mfuruya@yokohama-cu.ac.jp

Received 13 September 2012. Accepted for publication 16 December 2012.

Birt-Hogg-Dubé syndrome (BHD) is an autosomal dominant disorder caused by mutations in the gene mapped in the region of chromosome 17p11.2[1–3]. The protein encoded by this gene, namely folliculin (FLCN), is known to form a complex with its binding proteins, folliculin-interacting protein (FNIP)1 and FNIP2/FNIPL[4–6]. The FLCN complex interacts with 5′-AMP-activated protein kinase (AMPK)[4–6]. The affected family members with *FLCN* mutation have the risk of developing skin fibrofolliculomas, renal tumors and multiple pulmonary cysts that cause repeated pneumothorax[7]. The number of BHD families diagnosed by genetic testing has been increasing since the discovery of the *FLCN* gene in 2002[3], and there is a concern that still many undiagnosed patients miss the chance to have a medical examination for renal tumors.

Because BHD families are prone to developing tumors of the skin and kidney, *FLCN* is currently regarded as a tumor-suppressor gene[8]. Rodent models of BHD develop renal cysts, adenomas and carcinomas[9,10]. Somatic mutations and/or loss of heterozygosity (LOH) are required in the second copy of the *FLCN* gene for renal carcinogenesis[11]. On the other hand, LOH was not evident in BHD-associated fibrofolliculomas[12]. Bullous disorder in the lung had not been considered to be a neoplasm previously. In recent years, however, detailed histopathologic studies of resected lung specimens elucidated unique features of the cystic lesions; they are not overtly neoplastic, but are multifocally located as monolayer cysts composed of benign-looking pneumocytes[13,14]. In our studies of BHD lungs, cyst-lining epithelial cells were immunostained positively for FLCN[13,14]. These histopathologic analyses suggest that FLCN probably exists in a haploinsufficient form without somatic second hit mutations in the cyst-lining cells.

Intensive studies have improved our understanding of the signaling molecules that interact with FLCN. It is widely

accepted that FLCN interacts with AMPK and mammalian target of rapamycin (mTOR). The complex of hamartin (TSC1) and tuberin (TSC2), whose mutations lead to the systemic disorder named tuberous sclerosis complex (TSC), also interact with AMPK and mTOR complex 1 (mTORC1)[15]. Both TSC and BHD potentially cause disorders in the lung, skin and kidney. Therefore, BHD may be grouped into mTOR-associated hamartoma syndrome, as is TSC[15]. Dysregulated mTOR signaling has been investigated in FLCN-depleted conditions both *in vitro* and *in vivo*[6,9,16,17]. Although both stimulatory and inhibitory effects were reported using different models, a few *in vivo* studies using kidney-targeted FLCN knockout mice showed that mTOR signaling was activated under FLCN-depleted conditions in renal cysts[16,18]. In BHD patients' lungs, our recent immunohistochemical study indicates that phospho-mTOR (p-mTOR) and phospho-S6 ribosomal protein (p-S6) are mildly activated in the cyst-lining epithelial cells[14].

In the present study, we investigated the expression of mTOR signaling molecules in a case of BHD lung. This case showed a unique mutation pattern of *FLCN* in the intron acceptor site that had not been reported previously. The mutation resulted in the production of exon 6-skipped mRNA. We demonstrate the increases of some key molecules involved in mTOR signaling. This is the first report of semi-quantitative analysis of mTOR downstream molecules in human BHD lung.

MATERIALS AND METHODS

Samples

Written informed consent for analysis of the *FLCN* gene was obtained from the patient. The study was approved by the Institutional Review Boards (IRB) of Yokohama City University. The wedge resected lung tissues were the S3 and S6 portion of the left lobe that contained small cysts less than 1 cm in diameter. The part of resected lung tissue was frozen immediately in liquid nitrogen. The remaining tissue was fixed with 10% formalin and embedded in paraffin. Haematoxylin and eosin (HE) staining and Elastica van Gieson (EVG) stainings were done. Normal lung specimens from patients with other diseases were also used for RT-PCR, Western blotting and immunohistochemistry.

Antibodies

Rabbit polyclonal antibodies against FLCN (Santa Cruz Biotechnology, Santa Cruz, CA, USA), thyroid transcription factor-1 (TTF-1) (DAKO, Carpinteria, CA, USA) and prosurfactant protein C (proSP-C, Millipore, Bedford, MA, USA) were used for immunostaining. Rabbit monoclonal antibody against FLCN (Cell Signaling, Danvers, MA, USA) was used for Western blotting, and rabbit polyclonal antibodies against mTOR, phospho-mTOR (p-mTOR) (Ser2448), Akt, phospho-Akt (p-Akt) (Ser473) and phospho-S6 ribosomal protein (p-S6) (Ser235/236) (Cell Signaling), hypoxia-inducible factor-1α (HIF-1α) (Enzo, Farmingdale, NY, USA) and vascular endothelial growth factor (VEGF) (Abcam, Cambridge, UK) were used for both immunostaining and Western blotting.

Immunostainings

Immunohistochemistry was done using ENVISION kit (DAKO) and autoclave antigen retrieval technique. Working dilutions of the antibodies were 1:1000 for proSP-C, 1:200 for VEGF, 1:100 for TTF-1 and 1: 50 for others.

DNA isolation

DNA from peripheral blood leukocytes was obtained using LabPass Blood Mini kit (Cosmo GENETECH, Seoul, Korea) according to the manufacturer's instructions.

Direct sequencing

Exons of *FLCN* coding region (exon 4–14) were amplified by polymerase chain reaction (PCR) using the primers described previously[3]. The PCR conditions were as follows: at 95℃ for 5 min, 35 cycles at 96℃ for 5 s, 60℃ for 5 s, 68℃ for 3 s, with an extension step of 1 min at 72℃ at the end of the last cycle. After purification, DNA was labeled with Big Dye Terminator v1.1 Cycle Sequencing Kit (Applied Biosystems, Cleveland OH, USA) and DNA sequencing was done using a sequencer ABI Prism 3100 Genetic Analyzer (Applied Biosystems). In the region where nucleotide alteration was suggested, the PCR products were subcloned (TA Cloning Kit, Invitrogen, San Diego, CA, USA) and then sequenced to clarify the mutation pattern.

RNA isolation and RT-PCR

Total RNAs from frozen lung tissues were obtained using RNeasy Mini kit (QIAGEN, Tokyo, Japan) according to the manufacturer's instructions. The primers of reverse transcriptase-mediated PCR (RT-PCR) to examine the expression levels of human *FLCN* mRNA are as follows: forward 5′-CGGACATGTGCGAGGGCTGC-3′ and reverse 5′-GGAATGGCGTGAAGGCTGTG-3′[19]. Conditions for PCR

using the Fast cycling PCR kit (QIAGEN) were as follows: at 95℃ for 5 min, 35 cycles at 95℃ for 5 s, 60℃ for 5 s, 68℃ for 3 s, with an extension step of 1 min at 72℃.

Western blotting

The same amount proteins of cell lysates were electrophoresed on 12.5% SDS-PAGE and transferred to a PVDF membrane (Millipore). Horseradish peroxidase-conjugated goat anti-rabbit IgG (1:2500) was used as the secondary antibody. Bands were detected using an enhanced chemiluminescence system, according to the Hybond ECL protocol (GE Healthcare, Little Chalfont, UK).

RESULTS

Clinical history and FLCN gene mutation pattern

A 33-year-old Japanese female was admitted to our hospital for investigation of recurrent pneumothorax. The patient had pneumothorax for the first time at the age of 25, and then repeated pneumothorax seven times in the last 8 years. She had received video assisted thoracoscopic surgery (VATS) three times previously, and had been diagnosed as idiopathic blebs/bullae. She was a never smoker and did not have specific diseases such as endometriosis and alpha-1-antitrypsin deficiency. Her father and uncle also had episodes of pneumothoraces and her grandmother had pulmonary cysts (Fig. 1a).

Both computed tomography (CT) and thoracoscopy demonstrated bilateral pulmonary cysts localized predominantly at the subpleural regions of the lower lobes and perimediastinal regions (Fig. 1b,c). The patient received thorough medical examination. Typical fibrofolliculomas/trichodiscomas were not found in the face and neck, however, she had a 1 cm sized skin tumor in the right upper arm (Fig. 1d). She refused to receive skin biopsy for histopathologic analysis. It was noteworthy that her father had a similar skin tumor in the left forearm (Fig. 1e). Neither tumors nor cysts were found in the kidney. She subsequently underwent pulmonary wedge resection.

The resected lung tissues contained some un-ruptured cysts less than 1 cm in diameter. Microscopically, the specimen showed unique features; the cyst walls were composed in part of expanded alveolar wall and in another part of visceral pleura (Fig. 2a,b). Unlike idiopathic blebs/bullae, these un-ruptured cysts lacked active inflammation and fibrosis. A few cysts looked like giant alveoli. The inner surface of the cysts were lined by TTF-1-positive and proSP-C-positive pneumocytes (Fig. 2c,d), supporting the notion that they are epithelial-lining cysts[13]. To understand whether the previous pneumothorax was really caused by idiopathic blebs/bullae, we reviewed the histopathology of resected lung tissues operated two years ago in which ruptured cysts were included. Compared with un-ruptured lesions of the current tissue, ruptured cysts in the previous VATS tissue contained more hyperplastic and hyalinized pleurae (Fig. 2e). Mesothelial invagination was also observed, suggesting a feature of rupture-associated remodeling. Epithelial cells were detached from the inner surface, and thickened pleurae were morphologically indistinguishable from blebs/bullae. We observed, however, some unusual air spaces in the lung; an irregular-shaped wall composed of haphazardly dilated vessels separating two cystic lesions (Fig. 2f). Such vessels developed abnormally in size and shape. We hypothesized that the lesions are not idiopathic blebs/bullae, rather, that they may be hamartomatous cysts due to pathologic interaction between epithelial and mesenchymal components.

A point mutation at the acceptor site of intron 5

The pathologic features of the lung, together with the episode of repetitive pneumothorax, alerted us to the possibility of BHD. After obtaining informed consent and Institutional Review Board approval, genomic DNA was obtained from the patient's blood, and mutation analysis of the *FLCN* gene was performed. A point mutation was found in the acceptor site of intron 5 (c.397-1G>C) (Fig. 3a,b). No other mutation was detectable in exons 4–14. Cloning of the PCR products confirmed heterozygous point mutation at this site. This mutation is predicted to cause the skipping of exon 6. Therefore, mRNA was extracted from the frozen lung tissue, and RT-PCR was performed. When the sequence region between the exon 4 and exon 7 was amplified, RT-PCR showed two bands (Fig. 3c); one was normally a spliced band (453 bp) and another was a specific band that was not seen in normal lungs (231 bp). The normal and specific bands were extracted, respectively, and each PCR product was purified. Sequence analysis of the PCR products revealed the complete mRNA in the normal-sized band (Fig. 3d) and the short mRNA lacking exon 6 in the small-sized band (Fig. 3e). RT-PCR was also performed in the exon 4–5 and exon 9–13 fragments in which no mutation was detected. Only normal-sized bands were produced in both regions (data not shown).

The expression of FLCN and mTOR signaling molecules in the BHD lung

The involvement of FLCN in human pathophysiologic events is not fully understood. Both inhibitory and stimulatory effects of FLCN on mTORC1 have been demonstrated[6,9,16], and it is thought that the function of FLCN in mTOR signaling may be

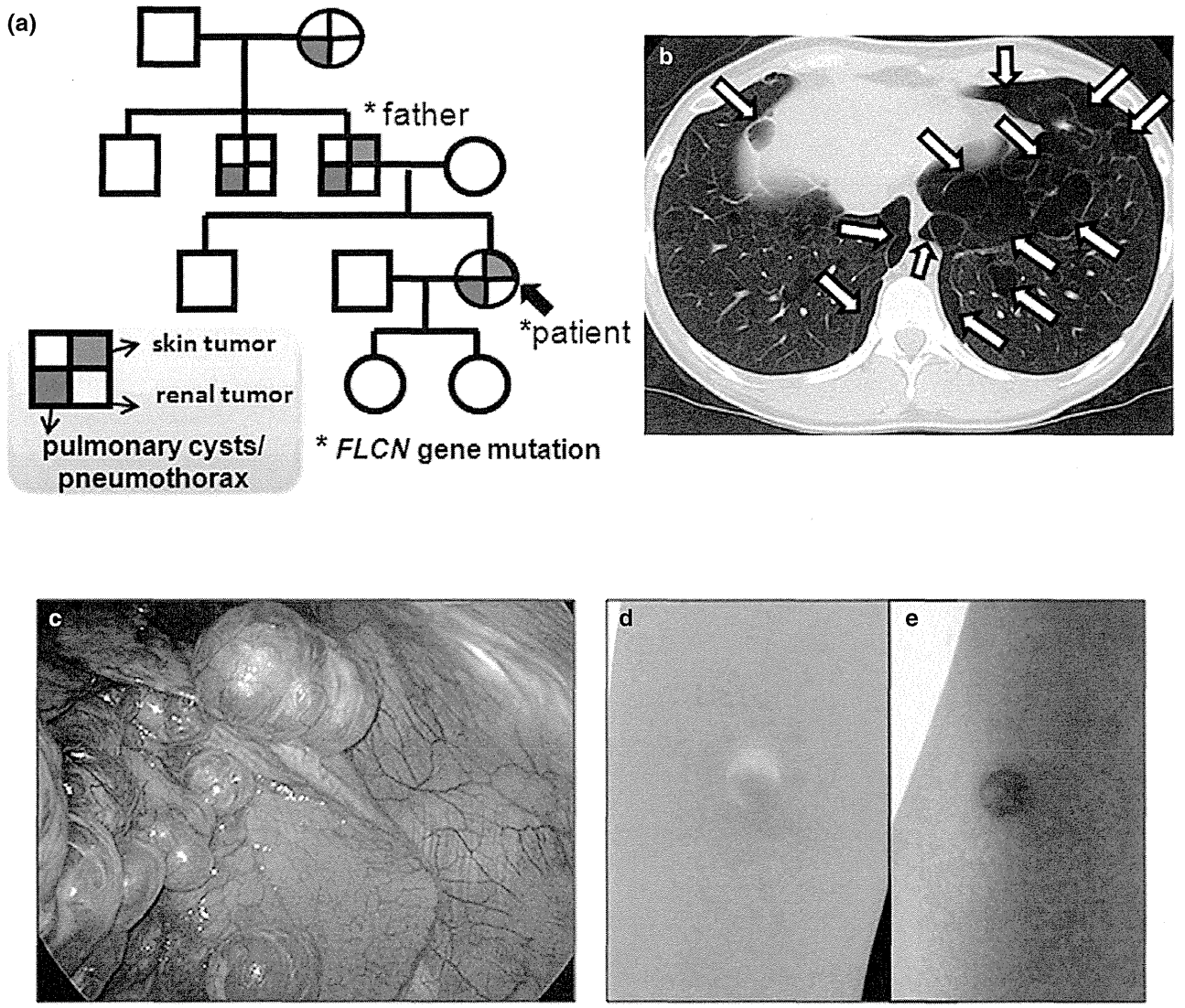

Figure 1 Inheritance of phenotypes, and radiologic and macroscopic findings. (**a**) Pneumothorax is the main manifestation of this family. The patient has repeated pneumothorax and multiple pulmonary cysts. Her father and uncle also have a history of pneumothorax. (**b**) Thoracic computed tomography of the patient's chest, indicating the predisposing condition to further rupture of the remaining cysts (arrows). (**c**) The thoracoscopy reveals multiple subpleural cysts in the lower lobe. (**d**) A skin tumor in the right upper arm of the patient, and (**e**) in the left forearm of the father.

context-dependent. In the current study, we investigated the signaling molecules involved in mTORC1 and mTORC2 pathways by Western blotting and immunohistochemical staining.

Protein was extracted from a portion of resected lung tissue, which contained both normal-looking parenchyma and microcystic lesions. In Western blotting analysis, the FLCN band was detectable in the BHD lung as well as in normal controls (Fig. 4a). Although the exon 6-skipped transcript was produced at mRNA level, we did not find any specific bands at protein level in this case. This result indicates that the exon 6-skipped transcript is either degenerated during protein synthesis or undetectable by the anti-FCLN antibodies we used in this study. Even though the FLCN depletion was not demonstrated at protein level, the bands of mTOR and p-mTOR (Ser2448) were significantly enhanced in the BHD lung compared with those in normal lungs (Fig. 4a). The downstream molecule p-S6 (Ser235/236) was also increased (Fig. 4a). Phosphorylated S6 is expected to work under the control of mTORC1 for protein synthesis. In addition to p-S6, we also found that the expression of p-Akt (Ser473), the downstream molecule of mTORC2, was enhanced in BHD lung (Fig. 4a). These results suggest that both mTORC1 and mTORC2 pathways

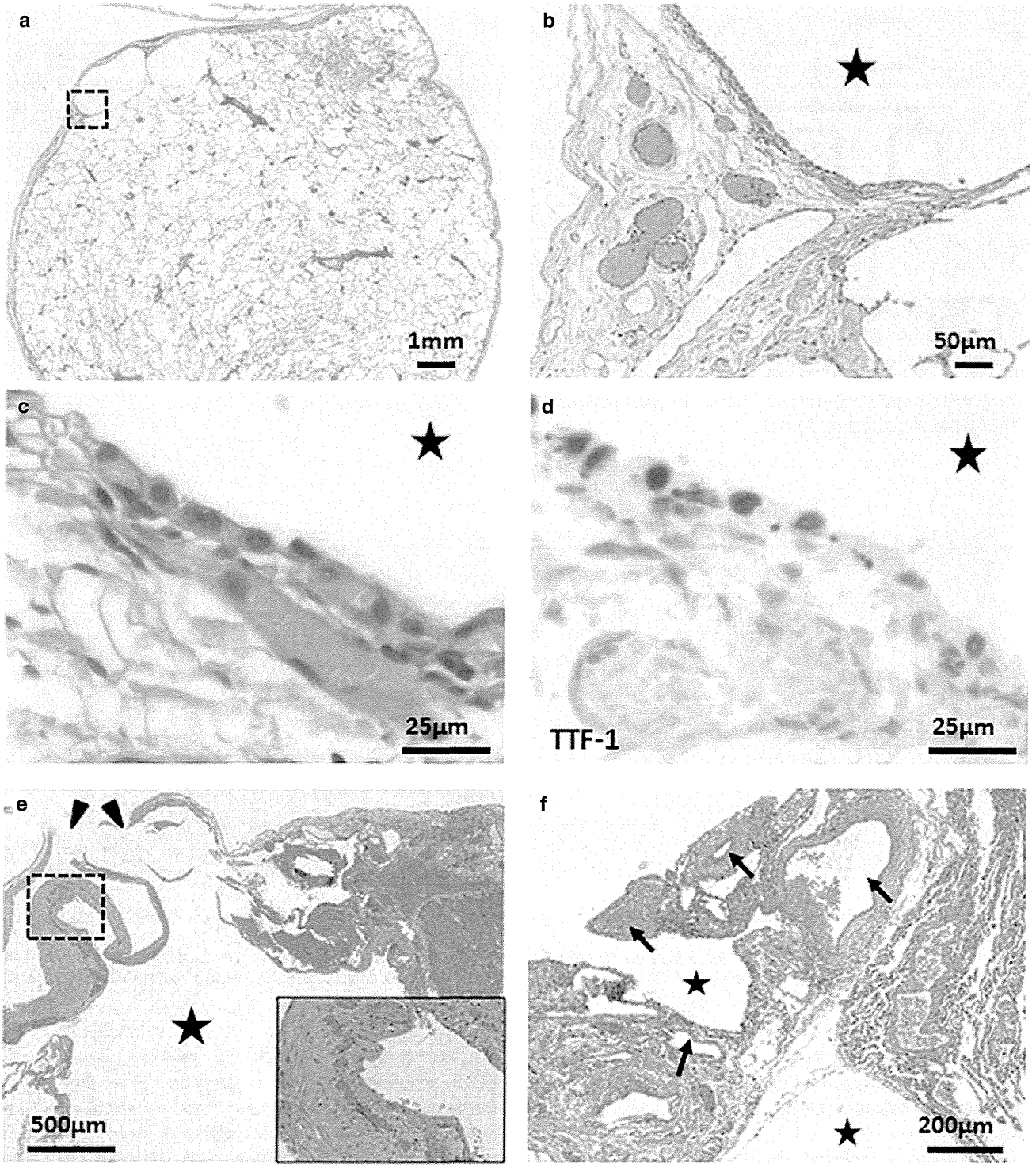

Figure 2 Histopathologic features of the resected lung: (**a**) Hematoxylin and eosin (HE) staining of the lung in the latest operation. The magnified region in (**b**) is indicated by a dotted rectangle. (**b**) Magnification of the cyst in (**a**). The cyst wall is fused to subpleura in outer side (upper left) and to alveoli in visceral side (right). A star indicates the lumen of Birt-Hogg-Dubé (BHD) cyst. (**c,d**) Higher magnification of the cyst shown in (**b**). Monolayer cells are lined in the inner surface (**c**), which are positively immunostained for thyroid transcription factor-1 (**d**). A star indicates the lumen of BHD cyst. (**e**) HE staining of the lung in the previous operation. Arrowheads indicate ruptured cyst wall. Hyalinized wall is indicated by a dotted rectangle. Inset: Higher magnification of the dotted lesion. A star indicates the lumen of BHD cyst. (**f**) Magnification of the interstitial septa located between two cysts. Distorted vessels are projected into the cyst lumen (arrows). Stars indicate the lumens of BHD cysts.

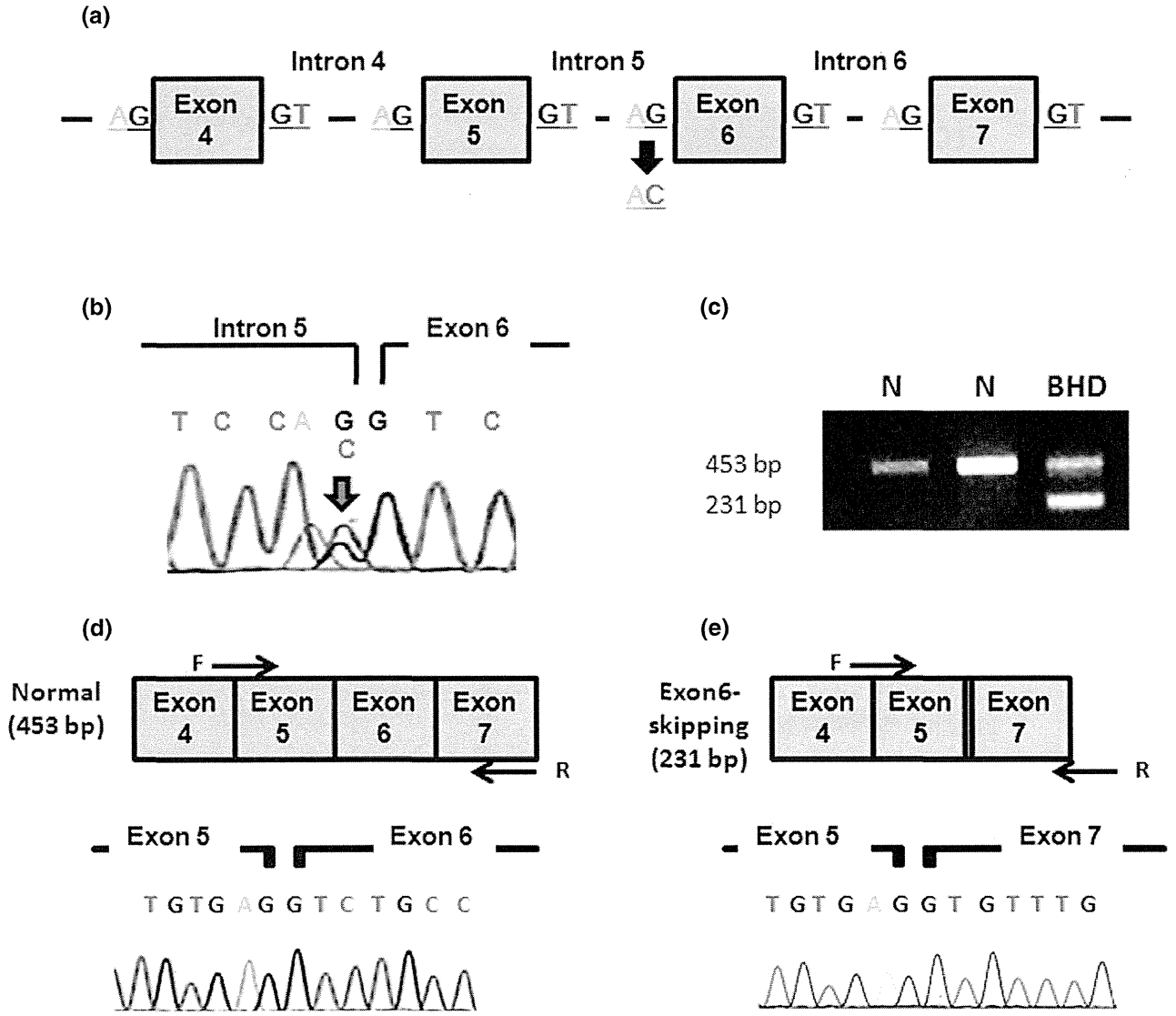

Figure 3 Analysis of *folliculin* gene mutation and *folliculin* mRNA. (**a**) A schema of *folliculin* (*FLCN*) gene. The 3′ end of intron 5 is mutated in this case. (**b**) Direct sequencing demonstrates the unique mutation pattern. The acceptor site of intron 5 is heterozygously mutated from AG to AC, indicated by an arrow. (**c**) mRNAs were extracted from the lung tissues, and transcriptase-mediated polymerase chain reaction (RT-PCR) was performed. PCR product samples were subjected to 2% agarose gel electrophoresis and visualized by staining with ethidium bromide. The upper bands (453 bp) indicate normally spliced PCR products, and the lower band in Birt-Hogg-Dubé lung (231 bp) indicates exon 6-skipped PCR product. (**d**), (**e**) Sequence analysis of *FLCN* gene transcripts in (**d**) normal and (**e**) the present cases. Exon 6-skipping is demonstrated in the present case. F and R indicate the forward and reverse primers, respectively. A red box indicates mutated 3′ end of intron 5.

are mildly activated in cysts of BHD lung under conditions of FLCN haploinsufficiency.

In immunostaining of mTOR molecules on the resected BHD lung tissues, both normal-looking pneumocytes and cyst-lining epithelial cells were positively immunostained for FLCN (Fig. 4b), which was consistent with the results of our previous histopathologic studies[13,14]. These cyst-lining cells were strongly immunostained for p-mTOR and p-S6, and weakly for p-Akt (Fig. 4c–e). In normal lungs ($n = 3$), p-mTOR and p-Akt were scarcely stained in pulmonary parenchyma, although weak immunostaining for p-S6 was observed in alveolar macrophages and bronchiolar epithelial cells. These results support the finding of Western blotting that the downstream molecules of mTORC1 and mTORC2 were activated in the BHD lung.

We noticed that the cyst walls contain many vessels. The subpleural lesions of ruptured cysts were hyalinized accompanied by bloody exudates and mesothelial invagination,

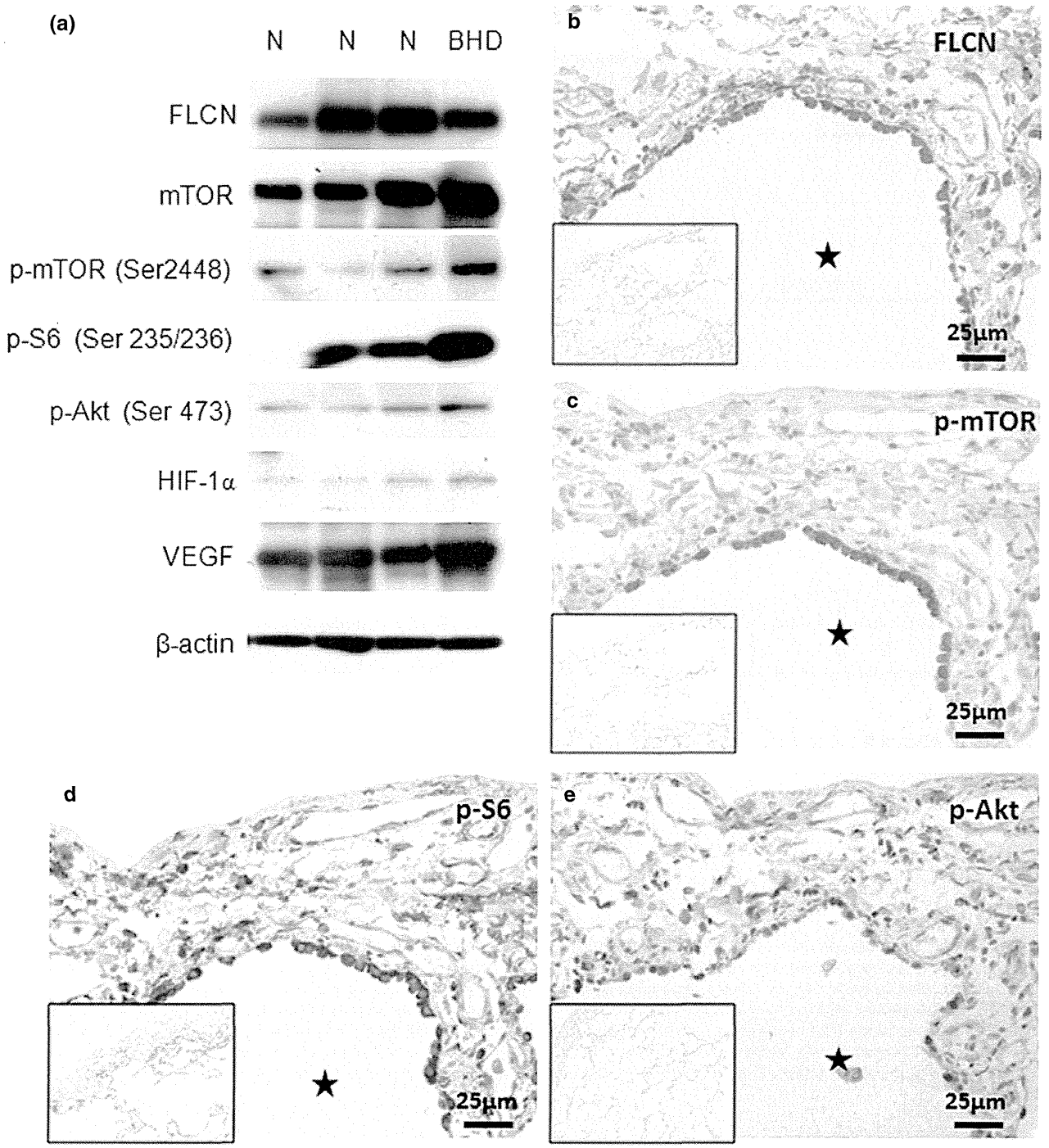

Figure 4 Expression of folliculin and mTOR signaling molecules in Birt-Hogg-Dubé lung. (**a**) Western blotting analysis of normal controls (N) and Birt-Hogg-Dubé (BHD) lung. The band of folliculin (FLCN) is detectable in BHD lung as strong as those in normal lungs. The band intensities of phospho-mTOR (p-mTOR), phospho-S6 ribosomal protein (p-S6), phospho Akt (p-Akt), hypoxia-inducible factor-1α (HIF-1α) and vascular endothelial growth factor (VEGF) are increased in BHD lung. (**b–e**), Immunostainings for (**b**) FLCN, (**c**) p-mTOR, (**d**) p-S6 and (**e**) p-Akt in the cyst of BHD lung using serial sections. Cyst-lining epithelial cells are significantly stained for these molecules. A star indicates the lumen of BHD cyst. Insets: Immunostainings for (**b**) FLCN, (**c**) p-mTOR, (**d**) p-S6 and (**e**) p-Akt in a normal control lung.

thus angiogenic vessels may reflect post-rupture remodeling (Fig. 2e). On the other hand, the subpleural layers of unruptured cysts had an increased number of small vessels without fibrotic remodeling (Fig. 5b, arrows), which was highlighted when compared with non-BHD control subpleurae (Fig. 5a). This finding indicates that the angiogenic cascade may be activated under the haploinsufficient condition of FLCN. We investigated HIF-1α, a downstream molecule of mTORC1. In Western blotting, the band of HIF-1α was enhanced (Fig. 4a). Consistently, immunohistochemical staining demonstrated the nuclear localization of HIF-1α in the cyst-lining cells (Fig. 5d), suggesting that the transcription of HIF-1α target genes are activated. Next, we investigated the expression of VEGF. HIF-1α is a well known transcriptional activator of VEGF. Compared with normal lungs, VEGF in BHD lung showed more intense band (Fig. 4a). In immunohistochemical staining, VEGF was strongly stained in the cyst-lining cells and endothelial cells of the wall (Fig. 5f). Such positive immunostaining was not observed in the subpleurae and parenchyma of normal lungs (Fig. 5c,e). The results suggest that the mTORC1 downstream angiogenic signaling is facilitated in the BHD lung.

DISCUSSION

More than 100 mutation patterns have been reported for the *FLCN* gene to date. Most of them are located in the exons containing coding sequences. In addition, several mutation sites in introns have been shown to be associated with pathogenic phenotypes. In the present study, we described a new mutation pattern at the intron 5 acceptor site. According to LOVD *FLCN* Mutation Database (http://grenada.lumc.nl/LOVD2/shared1), 12 mutation patterns have been reported in the intron donor/acceptor sites that are predicted to cause abnormal splicing. With regard to the intron 5 acceptor site, two mutation patterns have been reported among Japanese patients: c.397-10_397-1del[19] and c.397-7_399del[20]. The present case (c.397-1G>C), therefore, is the third Japanese BHD family with a unique mutation pattern at this site. As we and another group indicated previously, mutation-prone regions tend to be different between Japanese and Western BHD families[14,20]. This might explain in part phenotype-genotype correlation; BHD families of Western countries show skin tumors as a typical symptom, whereas most Japanese BHD patients exhibit repeated pneumothorax as the main or sole manifestation[19]. Some of Japanese BHD families show distinctive mutation patterns that have not been reported in Western countries, such as c.1347_1353dupCCCACCCT and c.1533_1536delGATG[13,19]. The intron 5 acceptor site may become another 'hot spot' for Japanese BHD families. Further studies are needed to understand whether they are pneumothorax-prone mutation patterns.

Some cases of BHD syndrome show mutations in intron acceptor sites that are expected to cause exon 10-, exon 11- and exon 13-skippings[12,20]. Gunji *et al.* demonstrated exon 6-skipped *FLCN* mRNA transcript using Epstein-Barr virus lymphoblastoid B cell line[19]. It had not been documented the condition of *FLCN* mRNA in the lung *in vivo*. In this case, we reveal for the first time that the affected patient's lung had exon 6-skipped *FLCN* mRNA transcript using freshly-frozen tissue. No clinical information is available at present on whether truncated proteins are actually produced in the pulmonary cysts of these cases. Exon 6-skipped *FLCN* mRNA transcript is expected to produce truncated FLCN that lacks 74 amino acids. We searched for abnormal-sized bands using two anti-FLCN antibodies from Cell Signaling and Santa Cruz, but could not find a candidate band (data not shown). One of the limitations of our study is that extracted protein from the lung contains both normal-looking parenchyma and microscopically cystic lesions in which most of lining cells exfoliated from cyst walls. Due to the small number of cyst-lining cells, we could not collect enough protein from the cyst by microdissection. Therefore, the possibility cannot be excluded that cyst-lining cells produce abnormal FLCN protein at very low level. Other possibilities include that predicted abnormal protein is unproductive or degenerative. It is likely that the structure of exon 6-depleted FLCN is not as stable as that of normal FLCN. Further investigations are needed to clarify whether exon 6-skipped *FLCN* mRNA actually produces truncated FLCN, or is eliminated *in vivo*.

All normal-appearing tissues of BHD affected individuals are under condition of FLCN haploinsufficiency, and only limited pulmonary areas develop cysts. Therefore, FLCN haploinsufficiency alone is unlikely to be enough to trigger cyst formation. Dysregulated mTOR signaling has been investigated in renal cysts and tumors of some rodent models and BHD patients[9,16,18,21]. Although it is not fully understood whether insufficient FLCN stimulates or suppresses mTOR pathway, some studies demonstrated an increase of downstream molecules in human BHD renal tumors such as S6 kinase and HIF-1α[21,22]. In the lung, we reported that the lining cells on the cysts were positively immunostained for p-mTOR and p-S6, suggesting that they are under activated conditions[14]. Since neoplastic proliferation is not evident in cyst-lining cells, the mTOR pathway may be less distinctively deviated in the pulmonary cysts than that in renal cell cancers.

The mechanisms of cyst development under condition of FLCN haploinsufficiency remain poorly understood. If accelerated mTORC1 signaling directly induces cystic remodeling, downstream molecules such as S6 ribosomal protein may play a key role. Only one report mentioned the molecule responsible for pulmonary cyst development, in which matrix metalloproteinase 9 (MMP9) was indicated to be involved in the affected lesion[23]. We examined the expression of MMP9, but did not find an increase of this enzyme in BHD lung (data

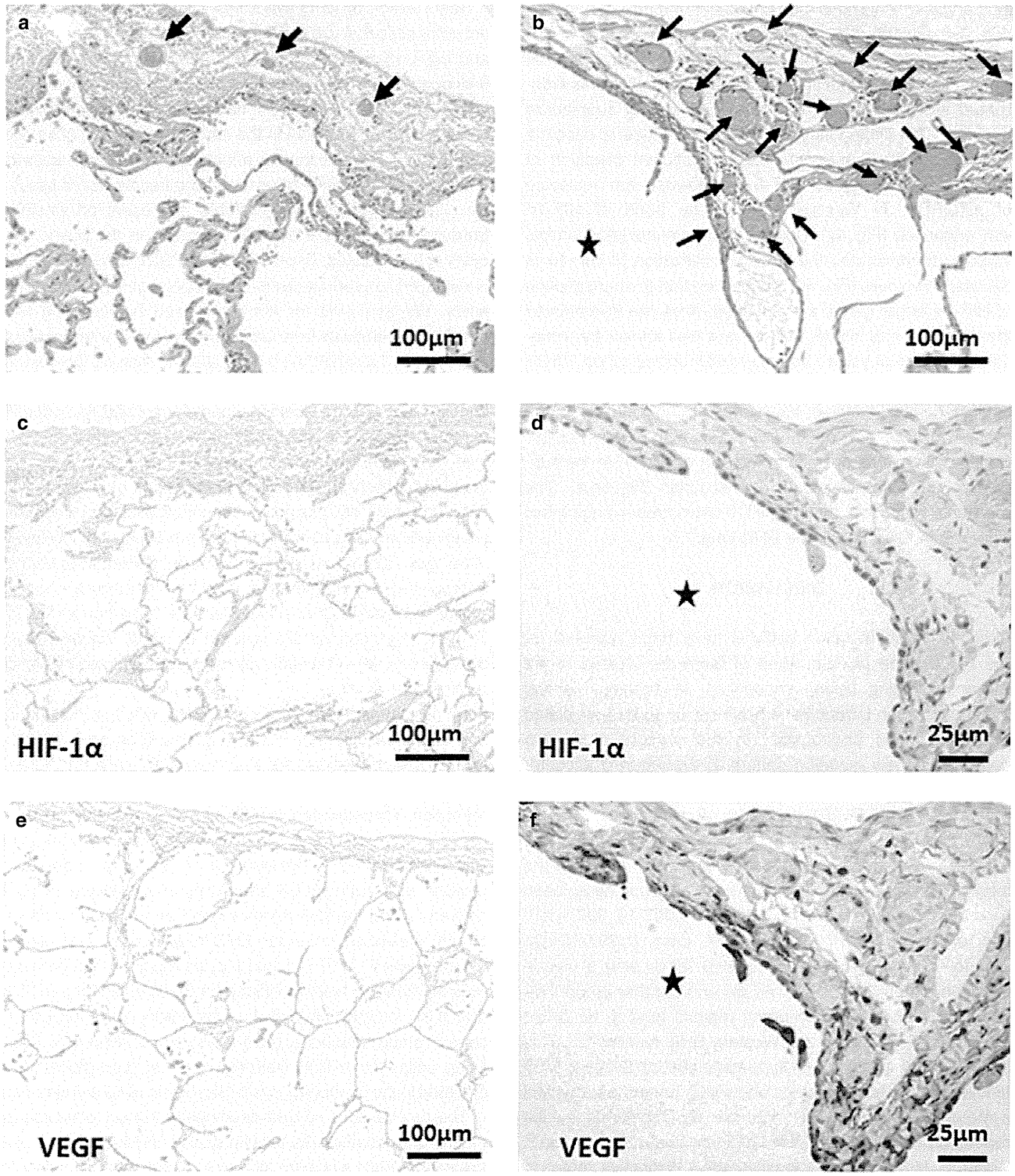

Figure 5 Angiogenic vessels in the cyst wall of Birt-Hogg-Dubé lung: (**a**) Hematoxylin and eosin (HE) staining of the subpleural area in a control lung. Only a few blood vessels are noted (arrows). (**b**) HE staining of the subpleural area in the un-ruptured Birt-Hogg-Dubé (BHD) cyst. The number of blood vessels is significantly increased (arrows). (**c,d**) Immunostainings for hypoxia-inducible factor-1α (HIF-1α) in normal lung and BHD cyst. (**d**) Strong nuclear staining for HIF-1α is observed in the cyst-lining cells, whereas (**c**) HIF-1α is negative in normal lung pneumocytes. (**e,f**) Immunostainings for vascular endothelial growth factor (VEGF) in normal lung and BHD cyst. (**f**) VEGF is strongly stained in the cyst-lining cells and vascular endothelial cells. (**e**) No significant VEGF staining is observed in normal lung pneumocytes and vessels. A star indicates the lumen of BHD cyst.

not shown). FLCN haploinsufficiency may affect not only epithelial cells but also mesenchymal components that support alveolar structure. In our immunohistochemical study, non-epithelial cells such as macrophages and vascular endothelial cells were also weakly stained for p-S6, HIF-1α and VEGF. Abnormal development of stromal components is well known in the polyps of Peutz-Jeghers syndrome, in which germline mutations of *LKB1/STK11* cause the activation of mTORC1[24]. This type of polyp can be developed in mice with mesenchymal-specific loss of *LKB1/STK11*[25]. Since BHD pulmonary cysts are closely incorporated with stroma, pathologic interaction between epithelium and mesenchyme should be investigated further.

HIF-1α is another downstream molecule of mTORC1 signaling, and it is one of the key molecules contributing to aberrant angiogenesis in many types of cancers. In this study, proliferation of blood vessels was noted in the vicinity of pulmonary cysts. Un-ruptured cysts did not show significant infiltration of immune cells. Therefore, inflammation-reactive angiogenesis, if any, is unlikely to be essential. Shear stress, such as cyst expansion and blood congestion around the cysts, may contribute to neovascularization. We propose another mechanism, namely, that the accelerated angiogenic signaling is owing in part to the increases of HIF-1α and VEGF associated with FLCN haploinsufficiency. Un-ruptured cyst walls of eight lung specimens previously diagnosed as BHD-associated pulmonary cysts[14] also demonstrated focal accumulation of small vessels in edematous stroma as seen in the current case (data not shown). These histopathologic findings support the notion that angiogenic signaling is activated, contributing to the development of BHD-associated pulmonary cysts. Further investigation is needed using larger number of cases whether the blood vessels around BHD cysts proliferate statistically.

Better understanding of pulmonary pathology of BHD syndrome will help us manage the affected patients who have the risks of developing tumors in the kidney and some other organs. This study suggests the involvement of FLCN haploinsufficiency in deranged mTOR signaling and downstream angiogenic activities in pulmonary cysts. mTOR inhibitors such as rapamycin and everolimus are reported to show efficacy in angiomyolipoma and lymphangioleiomyomatosis of TSC[26,27]. On the other hand, BHD lung has currently no effective therapy. We hope that our study will contribute to finding a new therapeutic approach by controlling mTOR and related pathways in BHD syndrome-associated multiple pulmonary cysts and repeated pneumothorax.

ACKNOWLEDGMENTS

The authors thank the members of respiratory disease center in Yokohama City University (YCU) Medical Center, and the members of pathology laboratories in YCU Medical Center and YCU Graduate School of Medicine for assistance. This work is supported by Grants in Aid for Scientific Research (M.F. and Y.N.).

REFERENCES

1 Khoo SK, Bradley M, Wong FK, Hedblad MA, Nordenskjold M, Teh BT. Birt-Hogg-Dube syndrome: Mapping of a novel hereditary neoplasia gene to chromosome 17p12-q11.2. *Oncogene* 2001; **20**: 5239–42.
2 Schmidt LS, Warren MB, Nickerson ML *et al.* Birt-Hogg-Dube syndrome, a genodermatosis associated with spontaneous pneumothorax and kidney neoplasia, maps to chromosome 17p11.2. *Am J Hum Genet* 2001; **69**: 876–82.
3 Nickerson ML, Warren MB, Toro JR *et al.* Mutations in a novel gene lead to kidney tumors, lung wall defects, and benign tumors of the hair follicle in patients with the Birt-Hogg-Dube syndrome. *Cancer Cell* 2002; **2**: 157–64.
4 Baba M, Hong SB, Sharma N *et al.* Folliculin encoded by the BHD gene interacts with a binding protein, FNIP1, and AMPK, and is involved in AMPK and mTOR signaling. *Proc Natl Acad Sci U S A* 2006; **103**: 15552–7.
5 Hasumi H, Baba M, Hong SB *et al.* Identification and characterization of a novel folliculin-interacting protein FNIP2. *Gene* 2008; **415**: 60–7.
6 Takagi Y, Kobayashi T, Shiono M *et al.* Interaction of folliculin (Birt-Hogg-Dube gene product) with a novel Fnip1-like (FnipL/Fnip2) protein. *Oncogene* 2008; **27**: 5339–47.
7 Toro JR, Wei MH, Glenn GM *et al.* BHD mutations, clinical and molecular genetic investigations of Birt-Hogg-Dube syndrome: A new series of 50 families and a review of published reports. *J Med Genet* 2008; **45**: 321–31.
8 Linehan WM, Srinivasan R, Schmidt LS. The genetic basis of kidney cancer: A metabolic disease. *Nat Rev Urol* 2010; **7**: 277–85.
9 Hartman TR, Nicolas E, Klein-Szanto A *et al.* The role of the Birt-Hogg-Dube protein in mTOR activation and renal tumorigenesis. *Oncogene* 2009; **28**: 1594–604.
10 Kouchi M, Okimoto K, Matsumoto I, Tanaka K, Yasuba M, Hino O. Natural history of the Nihon (Bhd gene mutant) rat, a novel model for human Birt-Hogg-Dube syndrome. *Virchows Arch* 2006; **448**: 463–71.
11 Vocke CD, Yang Y, Pavlovich CP *et al.* High frequency of somatic frameshift BHD gene mutations in Birt-Hogg-Dube-associated renal tumors. *J Natl Cancer Inst* 2005; **97**: 931–5.
12 van Steensel MA, Verstraeten VL, Frank J *et al.* Novel mutations in the BHD gene and absence of loss of heterozygosity in fibrofolliculomas of Birt-Hogg-Dube patients. *J Invest Dermatol* 2007; **127**: 588–93.
13 Koga S, Furuya M, Takahashi Y *et al.* Lung cysts in Birt-Hogg-Dube syndrome: Histopathological characteristics and aberrant sequence repeats. *Pathol Int* 2009; **59**: 720–8.
14 Furuya M, Tanaka R, Koga S *et al.* Pulmonary Cysts of Birt-Hogg-Dube Syndrome: A Clinicopathologic and Immunohistochemical Study of 9 Families. *Am J Surg Pathol* 2012; **36**: 589–600.
15 Inoki K, Corradetti MN, Guan KL. Dysregulation of the TSC-mTOR pathway in human disease. *Nat Genet* 2005; **37**: 19–24.
16 Baba M, Furihata M, Hong SB *et al.* Kidney-targeted Birt-Hogg-Dube gene inactivation in a mouse model: Erk1/2 and Akt-mTOR activation, cell hyperproliferation, and polycystic kidneys. *J Natl Cancer Inst* 2008; **100**: 140–54.

17 Hudon V, Sabourin S, Dydensborg AB *et al.* Renal tumour suppressor function of the Birt-Hogg-Dube syndrome gene product folliculin. *J Med Genet* 2010; **47**: 182–9.
18 Chen J, Futami K, Petillo D *et al.* Deficiency of FLCN in mouse kidney led to development of polycystic kidneys and renal neoplasia. *PLoS One* 2008; **3**: e3581.
19 Gunji Y, Akiyoshi T, Sato T *et al.* Mutations of the Birt Hogg Dube gene in patients with multiple lung cysts and recurrent pneumothorax. *J Med Genet* 2007; **44**: 588–93.
20 Kunogi M, Kurihara M, Ikegami TS *et al.* Clinical and genetic spectrum of Birt-Hogg-Dube syndrome patients in whom pneumothorax and/or multiple lung cysts are the presenting feature. *J Med Genet* 2010; **47**: 281–7.
21 Hasumi Y, Baba M, Ajima R *et al.* Homozygous loss of BHD causes early embryonic lethality and kidney tumor development with activation of mTORC1 and mTORC2. *Proc Natl Acad Sci U S A* 2009; **106**: 18722–7.
22 Preston RS, Philp A, Claessens T *et al.* Absence of the Birt-Hogg-Dube gene product is associated with increased hypoxia-inducible factor transcriptional activity and a loss of metabolic flexibility. *Oncogene* 2011; **30**: 1159–73.
23 Hayashi M, Takayanagi N, Ishiguro T, Sugita Y, Kawabata Y, Fukuda Y. Birt-Hogg-Dube syndrome with multiple cysts and recurrent pneumothorax: Pathological findings. *Intern Med* 2010; **49**: 2137–42.
24 Shaw RJ, Bardeesy N, Manning BD *et al.* The LKB1 tumor suppressor negatively regulates mTOR signaling. *Cancer Cell* 2004; **6**: 91–9.
25 Katajisto P, Vaahtomeri K, Ekman N *et al.* LKB1 signaling in mesenchymal cells required for suppression of gastrointestinal polyposis. *Nat Genet* 2008; **40**: 455–9.
26 Bissler JJ, McCormack FX, Young LR *et al.* Sirolimus for angiomyolipoma in tuberous sclerosis complex or lymphangioleiomyomatosis. *N Engl J Med* 2008; **358**: 140–51.
27 McCormack FX, Inoue Y, Moss J *et al.* Efficacy and safety of sirolimus in lymphangioleiomyomatosis. *N Engl J Med* 2011; **364**: 1595–606.

recipients [3, 4]. With better results and increased survival after transplantation, degenerative aortic valve disease, although not directly related to LTx or to immunosuppression after LTx per se, is to be increasingly expected in patients after transplantation as part of age-related pathologic processes. In the present case, aortic stenosis was diagnosed in our patient in his mid-60s, a decade after LTx.

Although AVR is performed as a routine procedure worldwide, the posttransplantation AVR candidate represents a unique cohort that needs management tailored to the individual's status after transplantation. Classic manifestations of cardiovascular disease may be masked or misattributed, or both, in a patient who has undergone transplantation. For example, dyspnea of heart failure may erroneously be attributed to declining pulmonary function resulting from infection or chronic allograft dysfunction. Hence, an important consideration in these patients is a high index of suspicion for codeveloping pathologic conditions, which should be screened for with relevant investigational modalities as appropriate. In this case, the patient's recent clinical findings of decreased exercise tolerance with chest tightness that was relieved by rest were initially attributed to a mild decline in his pulmonary function test results. Later events, however, bear testimony to the fact that early echocardiography might have yielded pertinent information, which prompts consideration of the interval and frequency at which patients who are apparently well after LTx, especially sexagenarians and elderly patients, should be screened for coexisting cardiovascular pathologic conditions. Nevertheless, a previous LTx need not be a deterrent to successful cardiac operations if the patient's lung function remains acceptable, as seen in our patient. Immunosuppressive drugs should be continued throughout through a nasogastric tube or intravenous route if necessary. The importance of maintaining adequate lung function perioperatively cannot be overemphasized—at our institute, the protocol is to check blood levels of immunosuppressants daily and adjust the dose as needed. These patients also warrant appropriate antibiotic therapy in view of their susceptibility to nosocomial/opportunistic infections. Prosthetic valve endocarditis occurred in a similar case of AVR in an LTx recipient [5]. Last, but not least, we believe that focused weaning of mechanical ventilation with a view to early extubation is a strategy that aids recovery of lung function in the immediate postoperative period, especially considering the potential for ventilator-associated pneumonia in immunosuppressed patients [6].

Transcatheter aortic valve implantation is becoming a valuable alternative to surgical AVR in nonoperable and high-risk surgical patients. However, the procedure has a potential for serious complications, and although short-term efficacy based on echocardiographic measurements is good, there are little data on long-term outcomes [7]. Our patient was considered for and given an option of transcatheter aortic valve implantation, but his age (early 60s), overall good general condition, and decent end-organ function prompted us to offer him a durable aortic valve prosthesis.

In conclusion, open heart surgical operations are a feasible option for cardiac disease in patients with acceptable lung function after LTx. Continuation of adequate immunosuppression, appropriate antibiotic cover, and early extubation constitute the cornerstones for successful surgical management of these patients.

References

1. Christie JD, Edwards LB, Kucheryavaya AY, et al. The Registry of the International Society for Heart and Lung Transplantation: twenty-seventh official adult lung and heart-lung transplant report—2010. J Heart Lung Transplant 2010;29:1104–18.
2. Gomez C, Reynaud-Gaubert M. Long-term outcome of lung transplantation. Rev Pneumol Clin 2010;67:64–73.
3. Kilic A, Merlo CA, Conte JV, Shah AS. Lung transplantation in patients 70 years old or older: have outcomes changed after implementation of the lung allocation score? J Thorac Cardiovasc Surg 2012;144:1133–8.
4. Tomaszek SC, Fibla JJ, Dierkhising RA, et al. Outcome of lung transplantation in elderly recipients. Eur J Cardiothorac Surg 2011;39:726–31.
5. Morsolini M, Zattera G, Meloni F, D'Armini AM. Aortic valve replacement performed twice through ministernotomy 15 years after lung transplantation. Ann Thorac Surg 2013;95:328–30.
6. Grgurich PE, Hudcova J, Lei Y, Sarwar A, Craven DE. Management and prevention of ventilator-associated pneumonia caused by multidrug-resistant pathogens. Expert Rev Respir Med 2012;6:533–55.
7. Yan TD, Cao C, Martens-Nielsen J, Padang R, Ng M, Vallely MP, Bannon PG. Transcatheter aortic valve implantation for high-risk patients with severe aortic stenosis: a systematic review. J Thorac Cardiovasc Surg 2010;139:1519–28.

FEATURE ARTICLES

Radiologically Indeterminate Pulmonary Cysts in Birt-Hogg-Dubé Syndrome

Takuya Onuki, MD, PhD, Yukinobu Goto, MD, PhD, Masami Kuramochi, MD, PhD, Masaharu Inagaki, MD, PhD, Ekapot Bhunchet, MD, PhD, Keiko Suzuki, MD, PhD, Reiko Tanaka, PhD, and Mitsuko Furuya, MD, PhD

Department of Thoracic Surgery, Tsuchiura Kyodo General Hospital, Tsuchiura; Department of Surgery (Thoracic Surgery), Faculty of Medicine, University of Tsukuba, Tsukuba; Department of Pathology, Tsuchiura Kyodo General Hospital, Tsuchiura; Medical Mycology Research Center, Chiba University, Chiba; and Department of Molecular Pathology, Yokohama City University Graduate School of Medicine, Yokohama, Japan

Birt-Hogg-Dubé (BHD) syndrome is an inherited disease characterized by recurrent pneumothorax. We report some unusual clinicopathologic features of the lung in a Japanese family with this syndrome presenting with recurrent pneumothorax. Radiologic imaging did not show

Accepted for publication May 17, 2013.

Address correspondence to Dr Onuki, 11-7 Manabe-shincho Tsuchiura, Ibaraki 300-0053, Japan; e-mail: onukitakuya@hotmail.com.

Published by Elsevier Inc
0003-4975/$36.00
http://dx.doi.org/10.1016/j.athoracsur.2013.05.120

detectable lesions; however, at video-assisted thoracic surgery (VATS), multiple diffusely distributed microcysts were visible on the pleura. This characteristic morphologic feature was common to all affected family members. The proband underwent genetic testing and BHD syndrome was diagnosed. Although many patients with BHD syndrome with pneumothorax show obvious pulmonary cysts, this case suggests that radiologically indeterminate cysts have the potential to cause pneumothorax.

(Ann Thorac Surg 2014;97:682–5)

Birt-Hogg-Dubé (BHD) syndrome is an autosomal dominant disease caused by mutation in the folliculin *(FLCN)* gene located on chromosome 17p11.2 [1]. The major features of this inherited disorder include recurrent pneumothorax, fibrofolliculomas, and renal cell cancer [2, 3]. All individuals with an episode of pneumothorax have multiple pulmonary cysts that can be identified by thoracic computed tomography (CT). Although previous studies have reported a possible association between the mutation patterns of *FLCN* and the frequency of pneumothorax [4, 5], the similarities in cyst morphologic features among the affected family members have not been well documented. In this report of familial recurrent pneumothorax, the family group consists of a female proband, who was diagnosed with BHD syndrome by genomic testing, and her 2 daughters. All 3 patients underwent video-assisted thoracic surgery (VATS). Thoracic CT did not demonstrate any cystic lesions; however, all 3 patients were found to have multiple microcysts on VATS, which was confirmed by pathologic examination.

A 52-year-old female nonsmoker presented to our institute with right-sided spontaneous pneumothorax. Five members of this family group had experienced spontaneous pneumothorax, including the patient's mother, cousin, and 2 daughters (Fig 1). The only information in the patients' medical histories that was of some significance was the repeated episodes of right-sided pneumothorax that generally resulted in mild symptoms. The patient consented to surgical intervention for diagnostic and therapeutic purposes. Preoperative thoracic CT showed no obvious cystic lesions (Fig 2A), which was considered unusual in the lung of a patient with spontaneous pneumothorax. At VATS, however, small thin-walled cystic structures were visible and were found to be diffusely distributed on the pleura of the right lung (Fig 2B). The patient underwent pulmonary wedge resection, cauterization using an Endo-FB3.0 Floating Ball (Medtronic, Inc, Minneapolis, MN), pleural ablation, and chemical pleurodesis a few days after operation. These are our standard surgical procedures for common spontaneous pneumothorax. Histopathologic examination of the resected tissue showed microcysts 4 mm in diameter (Fig 2B).

Because of the characteristic familial history of pneumothorax, BHD syndrome was suspected. DNA was obtained from peripheral blood leukocytes of the patient,

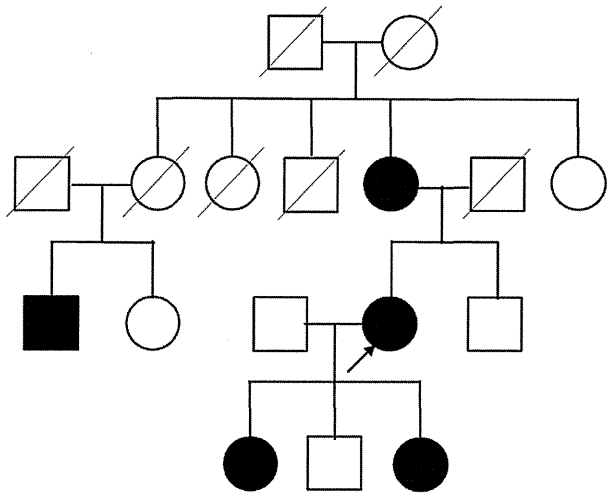

Fig 1. Pedigree chart. Proband is indicated by arrow. Filled boxes and circles indicate individuals with pneumothorax.

and exons of the *FLCN* gene were amplified by polymerase chain reaction: Direct sequences revealed a heterozygosis mutation in exon 12. The patient was finally

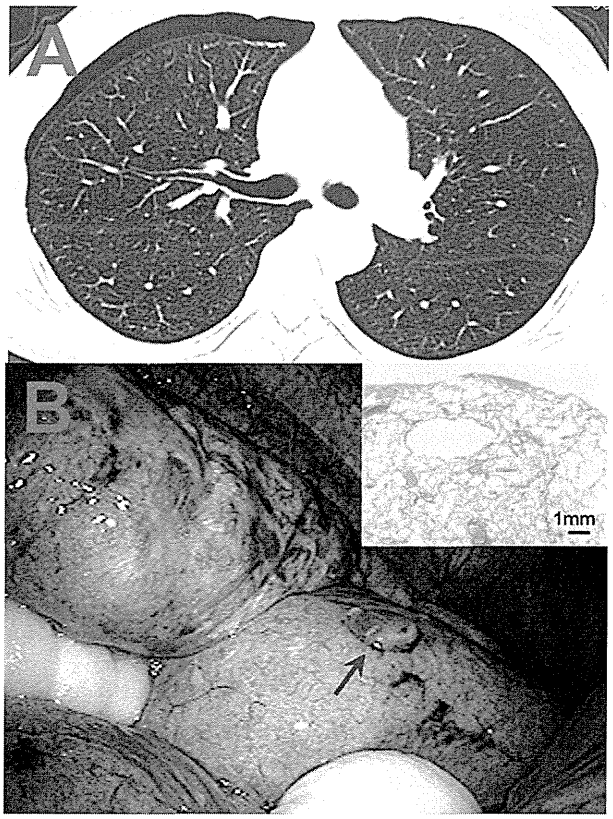

Fig 2. Intrathoracic findings of the proband. (A) Thoracic computed tomography fails to show any pulmonary cysts. (B) Intrathoracic findings for the patient. A tiny pulmonary cyst detected on the visceral pleura (arrow), is coagulated using Endo-FB3.0 Floating Ball. Resected pulmonary tissue contains a 4-mm-diameter microcyst (inset, hematoxylin and eosin stain).

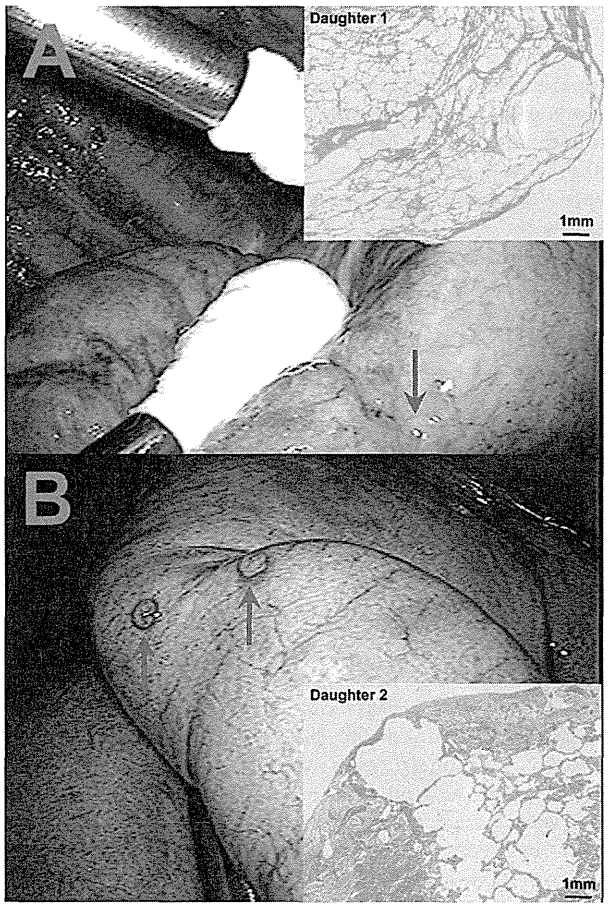

Fig 3. Intrathoracic findings for 2 daughters. (A) Daughter 1. (B) Daughter 2. Tiny pulmonary cysts are indicated by arrows. Microcysts are detected in each specimen (hematoxylin and eosin stain).

diagnosed with BHD syndrome. Neither fibrofolliculomas nor solid renal tumors were detected.

Interestingly, 2 of the patient's daughters had also undergone VATS for pneumothorax, and their clinical records are discussed here. Daughter 1 (D1) received VATS for right-sided spontaneous pneumothorax (Fig 3A) after 5 previous episodes of bilateral pneumothorax. She also presented postoperatively with recurrence of right-sided pneumothorax, which was treated with chemical pleurodesis. Daughter 2 (D2) received VATS for right-sided spontaneous pneumothorax (Fig 3B). Preoperative thoracic CT of D1 and D2 demonstrated no detectable pulmonary cysts, similar to their mother. In these cases, the surgical findings also resembled those seen in the mother, ie, small thin-walled cystic structures diffusely distributed over the pleura (Figs 3A, 3B). Histologic analysis of the resected pulmonary tissues from both daughters demonstrated microcysts. A catamenial cause of pneumothorax was ruled out, and although D1 and D2 did not consent to genetic testing for *FLCN*, the common clinicopathologic features in these cases strongly suggest that the *FLCN* mutation demonstrated in the proband was inherited by the daughters.

Comment

BHD syndrome was named after the study by Birt and colleagues [6] in 1977 describing a familial dermatologic disorder. The genetic test for this disorder was developed over the past decade [1]. The responsible gene has been identified as *FLCN*, which encodes the protein folliculin (FLCN). Repeated episodes of pneumothorax in adult patients aged 20 to 40 years is the key feature of BHD syndrome that warrants a thorough medical examination. In this unique study, 3 members of a family with BHD syndrome underwent surgical intervention and were followed at our institute, enabling comparison of detailed clinicopathologic findings. Notably, none of the individuals had pulmonary lesions determined by thoracic CT. Thoracoscopic and pathologic examinations identified microcystic lesions diffusely distributed over the pleura. To date, reports of BHD syndrome–associated pulmonary cysts and pneumothorax have not addressed whether the pulmonary lesions are similar in all affected family members. This study is the first to show that the pulmonary cysts in affected family members are pathologically similar. The pulmonary cysts of this family group were much smaller than those that have been reported previously [7]. This finding suggests that the size, morphologic features, and distribution patterns of the pulmonary cysts are inherited by the affected progeny. It has been reported that patients with BHD syndrome with a family history of spontaneous pneumothorax are significantly more likely to experience spontaneous pneumothorax than are those without a family history of spontaneous pneumothorax [4]. This indicates that the characteristic features of BHD syndrome differ between family groups. An important finding in this study is that microscopic cysts that are undetectable by thoracic CT have the potential to cause recurrent pneumothorax. In cases involving common spontaneous pneumothorax, we have often performed pleural ablation at VATS in combination with chemical pleurodesis a few days after operation, although these treatments would be not routinely carried out in other institutes. Chemical pleurodesis or pleural ablation in addition to standard surgical interventions are likely to be of even greater benefit in the treatment of pneumothorax caused by BHD syndrome, in which the cysts are diffusely distributed, than in common spontaneous pneumothorax.

In line with other recently published findings, these results help to further our knowledge about the pathologic characteristics and diagnosis of BHD syndrome–associated pulmonary cysts [7].

References

1. Nickerson ML, Warren MB, Toro JR, et al. Mutations in a novel gene lead to kidney tumors, lung wall defects, and benign tumors of the hair follicle in patients with the Birt-Hogg-Dubé syndrome. Cancer Cell 2002;2:157–64.

2. Schmidt LS, Nickerson ML, Warren MB, et al. Germline BHD-mutation spectrum and phenotype analysis of a large cohort of families with Birt-Hogg-Dubé syndrome. Am J Hum Genet 2005;76:1023–33.
3. Toro JR, Wei MH, Glenn GM, et al. BHD mutations, clinical and molecular genetic investigations of Birt-Hogg-Dubé syndrome: a new series of 50 families and a review of published reports. J Med Genet 2008;45:321–31.
4. Toro JR, Pautler SE, Stewart L, et al. Lung cysts, spontaneous pneumothorax, and genetic associations in 89 families with Birt-Hogg-Dubé syndrome. Am J Respir Crit Care Med 2007;175:1044–53.
5. Painter JN, Tapanainen H, Somer M, et al. A 4-bp deletion in the Birt-Hogg-Dubé gene (FLCN) causes dominantly inherited spontaneous pneumothorax. Am J Hum Genet 2005;76:522–7.
6. Birt AR, Hogg GR, Dubé WJ. Hereditary multiple fibrofolliculomas with trichodiscomas and acrochordons. Arch Dermatol 1977;113:1674–7.
7. Furuya M, Tanaka R, Koga S, et al. Pulmonary cysts of Birt-Hogg- Dubé syndrome: a clinicopathologic and immunohistochemical study of 9 families. Am J Surg Pathol 2012;36:589–600.

Two Unusual Cases of Adult Onset Congenital Bronchoesophageal Fistulas Treated With Fistula Division

Adamu Issaka, MD, Nezih O. Ermerak, MD, Volkan H. Kara, MD, PhD, Toni Lerut, MD, PhD, and Hasan F. Batirel, MD, PhD

Department of Thoracic Surgery, Marmara University Faculty of Medicine, Istanbul, Turkey; and Department of Thoracic Surgery, University Hospital Gasthuisberg, Leuven, Belgium

Adult onset congenital bronchoesophageal fistula is a very rare entity. We report 2 cases of adult onset type II congenital bronchoesophageal fistula between the distal thoracic esophagus and the lower lobe superior segmental bronchi surgically treated through a right and left thoracotomy, respectively. In both cases the fistula was transected and sutured with no parenchyma resection. Both patients had an uneventful recovery. Resection of the underlying parenchyma during surgery for bronchoesophageal fistula is not always necessary as the lung can heal in time after performing just fistulectomy.

(Ann Thorac Surg 2014;97:685–7)

Bronchoesophageal fistula (BEF) is an abnormal communication between the esophagus and the bronchial tree. It can be acquired or congenital. Congenital BEF when associated with esophageal atresia presents early in life. In the absence of coexisting esophageal malformations symptoms may not present until adult life and is often intermittent. Congenital BEF in adult life is rare and most literature comprise of case reports [1, 2]. Most reported literature advocate fistulectomy and resection of the underlying parenchyma. We report the surgical treatment of 2 cases of adult onset BEF where we preserved the underlying parenchyma with both patients having a well expanded lung during follow-up.

The first patient was a 39-year-old male and the second, a 55-year-old female. Both patients had symptoms of bouts of cough when swallowing liquids since childhood. Barium swallow was diagnostic in both patients showing a fistula tract between the esophagus and the lower lobe bronchi (Fig 1). Chest computed tomography scan revealed consolidations and atelectasis in the right lower lobe superior segment, and infiltrations in the left lower lobe superior segment, respectively. Both patients were operated through a thoracotomy. In the first patient bronchoscopy and esophagoscopy confirmed the orifices of the fistula, whereas in the second patient only bronchoscopy revealed the fistula in the left lower lobe superior segmental bronchus. Both patients underwent thoracotomy and had significant adhesions in their lower lobes. Careful dissection of the posterior mediastinal pleura from the level of the carina to the inferior pulmonary vein was done. Large collateral vessels were noticed on the aorta in the female patient. The fistula tract was just above the inferior pulmonary vein between the esophagus and the lower lobe superior segmental bronchi (Fig 2).

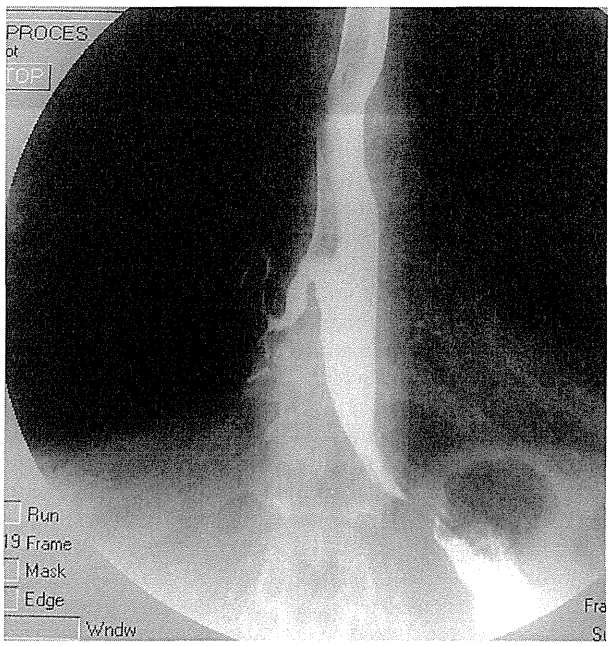

Fig 1. Barium swallow showing fistula between esophagus and right lower lobe superior segmental bronchus in the male patient.

Accepted for publication June 3, 2013.

Address correspondence to Dr Batirel, Marmara University Hospital, Thoracic Surgery Department, 7. Kat, Gogus Cerrahisi. Fevzi Cakmak Mah., Mimar Sinan Cad., No: 41, 34899, Ust Kaynarca, Pendik, Istanbul, Turkey; e-mail: hbatirel@marmara.edu.tr.

0003-4975/$36.00
http://dx.doi.org/10.1016/j.athoracsur.2013.06.111

ARTICLE IN PRESS

Annals of Diagnostic Pathology xxx (2014) xxx–xxx

Contents lists available at ScienceDirect

Annals of Diagnostic Pathology

Original Contribution

Intratumoral peripheral small papillary tufts: a diagnostic clue of renal tumors associated with Birt-Hogg-Dubé syndrome☆,☆☆

Naoto Kuroda, MD [a,*], Mitsuko Furuya, MD [b], Yoji Nagashima, MD [b], Hiroko Gotohda, MD [c], Suzuko Moritani, MD [d], Fumi Kawakami, MD [e], Yoshiaki Imamura, MD [f], Yoshimi Bando, MD [g], Masayuki Takahashi, MD [h], Hiro-omi Kanayama, MD [h], Satoshi Ota, MD [i], Michal Michal, MD [j], Ondrej Hes, MD [j], Yukio Nakatani, MD [i]

[a] Department of Diagnostic Pathology, Kochi Red Cross Hospital, Kochi, Japan
[b] Department of Molecular Pathology, Yokohama City University Graduate School of Medicine, Yokohama, Japan
[c] Division of Pathology, JA Hokkaido Koseiren Sapporo Kosei Hospital, Sapporo, Japan
[d] Department of Advanced Diagnosis, Division of Pathology, Nagoya Medical Center, Nagoya, Japan
[e] Department of Diagnostic Pathology, Kobe University Hospital, Kobe, Japan
[f] Division of Surgical Pathology, University of Fukui Hospital, Fukui, Japan
[g] Division of Pathology, Tokushima University Hospital, Tokushima, University of Tokushima Graduate School, Tokushima, Japan
[h] Department of Urology, Institute of Health Biosciences, University of Tokushima Graduate School, Tokushima, Japan
[i] Department of Diagnostic Pathology, Chiba University Graduate School of Medicine, Chiba, Japan
[j] Department of Pathology, Charles University in Prague, Faculty of Medicine, Plzen, Czech Republic

ARTICLE INFO

Available online xxxx

Keywords:
Intratumoral peripheral small papillary tufts
Renal tumor
Birt-Hogg-Dubé syndrome

ABSTRACT

In this article, we searched for the common histologic characteristic of renal tumors in patients with Birt-Hogg-Dubé syndrome (BHDS). We selected 6 patients with histologically confirmed renal tumor in BHDS. Germline *FLCN* gene mutation has been identified in 5 patients. Multifocality and bilaterality of the renal tumors were pathologically or radiologically confirmed in 5 and 2 cases, respectively. Histologic subtypes of the dominant tumor included 3 previously described hybrid oncocytic tumors, one composite chromophobe/papillary/clear cell renal cell carcinoma (RCC) and one unclassified RCC resembling hybrid chromophobe/clear cell RCC. In one case, chromophobe RCC and clear cell RCC were separately observed. Small papillary lesions located in the peripheral area of the tumor, which we designated as intratumoral peripheral small papillary tufts, were identified in all patients. In conclusion, multifocality/bilaterality of renal tumors, discordance of histologic subtypes, and the presence of intratumoral peripheral small papillary tufts may be important clues to identify BHDS-associated renal tumors.

1. Introduction

Birt-Hogg-Dubé syndrome (BHDS) is an autosomal dominant hereditary disease characterized by the association of skin lesions, such as fibrofolliculoma, trichodiscoma, and acrochordon of the face, neck, and upper trunk, pulmonary lesion including cyst and spontaneous pneumothorax and renal tumors [1,2]. BHDS–associated renal tumors are characterized by multiplicity and bilaterality and the histologic subtypes including hybrid oncocytic tumor called as hybrid oncocytic/chromophobe tumor (HOCT), chromophobe renal cell carcinoma (RCC), oncocytoma, clear cell RCC, and papillary RCC [1,3-9]. Currently, we had the opportunity to observe the characteristic present in all tumors in our series. In this article, we report an important diagnostic clue of BHDS-associated renal tumors, intratumoral peripheral small papillary tufts (ITPSPT) and discuss its significance.

2. Materials and methods

2.1. Study design

This study was permitted by Ethical Committee (no. 129) at Kochi Red Cross Hospital, Kochi, Japan. We present 6 cases of histologically diagnosed BHDS-associated renal tumors selected from 398 cases renal tumors of consultation files of Department of Diagnostic Pathology, Kochi Red Cross Hospital between January 2010 and October 2013. Three cases including one family history of mother and daughter have previously been reported [10,11].

☆ Conflict of interest: None.

☆☆ This study was in part supported by a grant-in-aid from the Japanese Ministry of Welfare and Labor (to MF and YN).

* Corresponding author: Department of Diagnostic Pathology, Kochi Red Cross Hospital, Shin-honmachi 2-13-51, Kochi City, Kochi 780-8562, Japan. Tel.: +81 88 822 1201; fax: +81 88 822 1056.
E-mail address: kurochankochi@yahoo.co.jp (N. Kuroda).

http://dx.doi.org/10.1016/j.anndiagpath.2014.03.002
1092-9134/

Please cite this article as: Kuroda N, et al, Intratumoral peripheral small papillary tufts: a diagnostic clue of renal tumors associated with Birt-Hogg-Dubé syndrome, Ann Diagn Pathol (2014), http://dx.doi.org/10.1016/j.anndiagpath.2014.03.002

Table 1
Clinical summary of 6 cases with BHDS.

Case	Age	Sex	MF	BL	Follow-up (mo)	Outcome	Other findings
1	69	F	+	−	46	AWOD	pulmonary cyst, skin lesion
2	46	F	−	−	37	AWOD	pulmonary cyst
3	67	M	+	−	26	AWOD	pulmonary cyst, pneumothorax
4	54	M	+	+	20	AWOD	pulmonary cyst
5	63	M	+	−	10	AWOD	Pulmonary cyst, fibrofolliculoma
6	66	F	+	+	13	AWOD	pulmonary cyst, skin lesion (sebaceous hyperplasia)

Abbreviations: *F*, female; *M*, male; *MF*, multifocality; *BL*, bilaterality; *AWOD*, alive without disease.
Cases 1 and 2 belong to the same family.

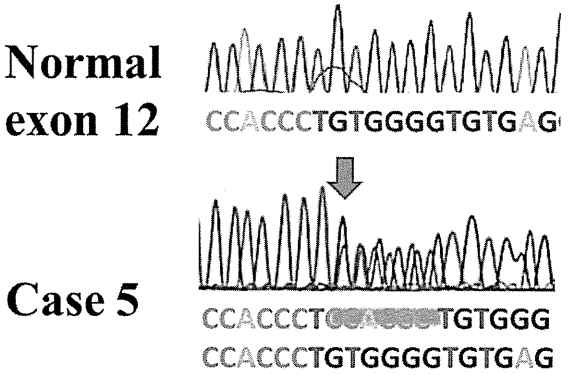

Fig. 1. *FLCN* gene mutational analysis. In exon 12, the mutation of c.1347_1353dupCCACCCT (arrow) is noted.

2.2. FLCN gene mutational analysis

Samples obtained from peripheral blood leucocytes of 5 cases (1-5) were used for genetic confirmation of germline mutation of *FLCN* gene at Department of Molecular Pathology, Yokohama City University Graduate School of Medicine. Molecular genetic study was performed according to the previously described method [11]. Briefly, genomic DNA was isolated from peripheral blood leukocytes using Lab Pass Blood Mini kits (Cosmo GENETECH, Seoul, Korea) according to the manufacturer's protocols. For direct sequencing, 14 exons of the *FLCN* gene were amplified by polymerase chain reaction (PCR) using the previously described primers [12]. The conditions of PCR were performed as previously reported [13]. After purification, DNA was labeled with the BigDye Terminator v1.1 Cycle Sequencing Kits (Applied Biosystems Cleveland, OH), and DNA sequencing was carried out using the ABI Prism 3100 Genetic Analyzer (Applied Biosystems). The PCR products from presumptive regions of nucleotide alterations were subcloned (TA Cloning Kit; Invitrogen, San Diego, CA) and then sequenced to elucidate the mutation patterns.

FLCN gene mutation in the paraffin block tissue of one case (1) was also examined at Department of Pathology in Charles University in Prague, Faculty of Medicine in Plzen.

Written informed consents were obtained from all the patients involved in current study.

2.3. Histologic and immunohistochemical examinations

The first levels of histologic sections were cut from formalin-fixed and paraffin-embedded tissue blocks and stained with hematoxylin and eosin. The subsequent levels of tissue sections were cut for the identification of immunohistochemical phenotype of ITPSPT and stained with Ventana Benchmark XT autostainer (Ventana Medical Systems, Tucson, AZ). The primary antibodies against CD82 (G-2, 1:200; Santa Cruz Biotechnology, Inc, CA), CD10 (56C6, prediluted; Novocastra Laboratories Ltd, Newcastle, UK), RCC Marker (PN-15, prediluted; Cell Marque, CA), E-cadherin (NCH-38, 1:100; Dako, Glostrup, Denmark), cytokeratin 7 (OV-TL 12/30, 1:800; Dako), and carbonic anhydrase 9 (CA9) (D47G3, 1:200; Cell Signaling Technology, MA) were used in the present study.

Table 2
Genetic findings of 6 cases with BHDS.

Case	*FLCN* gene mutation
1	Exon 5 c.332_349del
2	Exon 5 c.332_349del
3	Exon 11 c.1285dupC
4	Exon 13 c.1533-1536 delGATG
5	Exon 12 C.1347-1353 dupCCACCCT
6	Not performed

3. Results

3.1. Clinical features

The clinicopathologic data are summarized in Table 1. This study included 3 males and 3 females. The patient age at diagnosis ranged from 46 to 69 years with a mean age of 60.8 years. The specimens were reviewed, and final histologic diagnosis was determined by 2 pathologists (NK and YN). Regarding diseases associated with BHDS, all patients had pulmonary cyst, and one patient had a history of spontaneous pneumothorax. Skin lesions were present in 3 patients.

3.2. Clinical outcome

These results are summarized in Table 1. The follow-up period ranged from 10 to 46 months with mean period 5.3 months. Neither recurrence nor metastases were noted.

3.2.1. Molecular genetic study of germline mutation of FLCN gene

Results are summarized in the Table 2. In all 5 cases examined, mutations of *FLCN* gene, including 2 cases in exon 5, one case in exon 11, one case in exon 12, and one case in exon 13, were observed (Fig. 1).

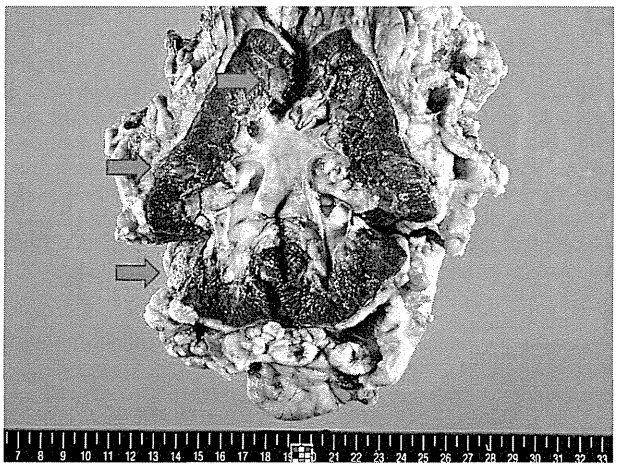

Fig. 2. Macroscopic findings of the kidney associated with BHDS. Multiple tumors (arrows) are observed.

Please cite this article as: Kuroda N, et al, Intratumoral peripheral small papillary tufts: a diagnostic clue of renal tumors associated with Birt-Hogg-Dubé syndrome, Ann Diagn Pathol (2014), http://dx.doi.org/10.1016/j.anndiagpath.2014.03.002

Table 3
Pathologic and genetic findings of 6 cases with BHDS.

Case	ITPSPT	MOC/ MCC	Dominant tumor	Detail of dominant tumor
1	+	MOC	Unclassified	Resembling hybrid chromophobe/clear cell RCC
2	+	–	HOCT	
3	+	MCC	Composite tumor	Collision of chromophobe RCC, clear cell RCC, and papillary RCC, type 1
4	+	MOC	HOCT	
5	+	MCC	Chromophobe RCC & clear cell RCC	2 tumors are separately present
6	+	–	HOCT	

Abbreviations: *MOC*, microscopic oncocytic change; *MCC*, microscopic clear cell change.

3.2.2. Radiologic or macroscopic findings

Among 6 patients, multiplicity and bilaterality was pathologically or radiologically confirmed in 5 and 2 cases, respectively (Fig. 2) (Table 1).

3.2.3. Histologic findings

Pathologic findings are summarized in Table 3. The dominant tumor included 3 HOCTs (cases 2, 4, and 6) previously described (4), one composite chromophobe RCC/papillary/clear cell RCC (Fig. 3A) with small papillary tufts at the interface between area of chromophobe and clear cell RCCs (case 3) (Fig. 3B), and one unclassified RCC resembling hybrid chromophobe/clear cell RCC (case 1). In one case, chromophobe RCC and clear cell RCC were separately identified (case 5) (Fig. 3C and D). Small papillary lesions were identified predominantly in the peripheral area of the tumor in all cases (Fig. 3E). We designated this characteristic morphologic sign as ITPSPT. Glandular lumens, typical of ITPSPT, were elongated or dilated and extended toward the central portion of the tumor in case 6 (Fig. 3F). ITPSPT were also observed at the interface of the tumor and normal renal parenchyma (Fig. 3G). Perinuclear halo and binucleation were identified at the higher magnification of several lesions (Fig. 3H). Oncocytic differentiation (Fig. 4A) and clear cell differentiation (Fig. 4B) in the renal parenchyma were noted in 2 (cases 1 and 4) and 2 cases (cases 3 and 5), respectively. These lesions seemed to be focally mixed. In case 1, 2 papillary adenomas were present (Fig. 4C). Small papillary tufts reminiscent of ITPSPT were identified in the grossly normal-looking renal parenchyma of case 1 (Fig. 4D). In addition, small chromophobe-like lesions with cystic change and focal papillary configuration were identified in one case (case 4) (Fig. 4E). At high magnification, shrunken nuclei, perinuclear halo, and prominent cell membranes were confirmed in this lesion (Fig. 4F). Immunohistochemical results are summarized in Table 4. ITPSPT were diffusely positive for CD82 (Fig. 5A), cytokeratin 7 (Fig. 5B), and E-cadherin in all examined cases but were negative for CD10, RCC, and CA9 in all tested cases.

4. Discussion

Patients with BHDS have an approximately 7-fold increased risk for renal neoplasia [3,14]. BHDS–associated renal tumors occur before or around the age of 50 years, but earlier onset in 20s has also been reported [9,14,15]. However, we found only one case before the age of 50 years in the present study. Hence, pathologists and urologists should bear in mind that BHDS-associated renal tumors in Japan often occur in the late onset. The estimated penetrance of renal cancer in *FLCN* gene mutation carriers is 16% at the age of 70 years [9]. Renal tumors associated with BHDS usually occur as multiple and bilateral lesions. These tumors demonstrate a wide histologic spectrum including HOCT, characterized by histologic features of both chromophobe RCC and oncocytoma with/without clear cell change, chromophobe RCC, oncocytoma, clear cell RCC, and papillary RCC [1,3-9]. In the present study, 50% of histologic subtypes of the main tumor mass were diagnostically consistent with HOCT. Such results were similar to the previously reported series [4]. The histologic concordance in patients with BHDS is lower than those with non-BHDS [16]. The histologic discordance of the main tumors including composite and separate tumors was confirmed in 2 cases (3 and 5). Cases with combined clear cell RCC/papillary RCC, hybrid chromophobe/clear cell RCC, papillary RCC with oncocytic change, and RCC with sarcomatoid change have been described in previous studies [9,17,18]. Accordingly, pathologists should be aware that such hybrid tumor or composite (collision) renal tumors might be diagnostic clue of BHDS. Oncocytosis is observed in 58% of patients histologically [2,4,19]. This lesion should be strictly distinguished from renal oncocytosis associated with renal failure/hemodialysis or of sporadic type of oncocytosis based on

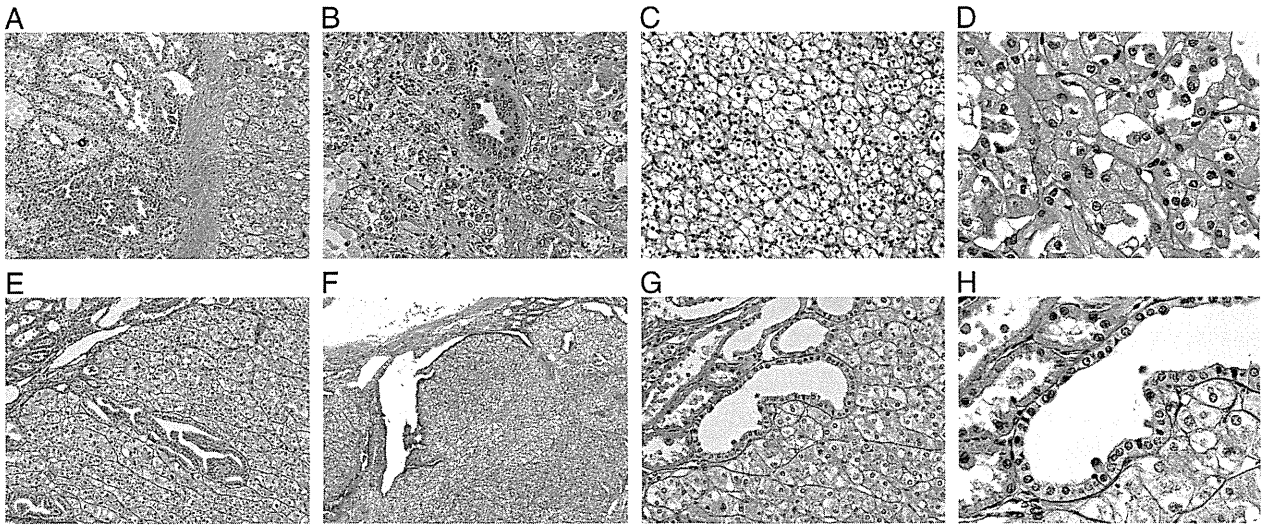

Fig. 3. Microscopic findings of the dominant renal lesions associated with BHDS. (A), In case 3, areas of chromophobe RCC, clear cell RCC, and papillary RCC, type 1 are collided with each other. (B), In case 3, small papillary tufts (center) is observed between chromophobe RCC and clear cell RCC. (C), In one tumor of case 4, clear cell RCC is seen. (D), Chromophobe RCC characterized by thick cell border, shrunken nuclei, and perinuclear halo is noted in another tumor of case 4. (E), Small papillary tufts, designated as ITPSPT, are observed. (F), Larger lesion of ITPSPT in case 6. Glandular lumens are elongated and dilated and extend into the central portion of the tumor. (G), ITPSPT are seen at the interface of the tumor and normal parenchyma. (H), Higher magnification of (G). ITPSPT have perinuclear halo, binucleation, and thick cell border.

Please cite this article as: Kuroda N, et al, Intratumoral peripheral small papillary tufts: a diagnostic clue of renal tumors associated with Birt-Hogg-Dubé syndrome, Ann Diagn Pathol (2014), http://dx.doi.org/10.1016/j.anndiagpath.2014.03.002

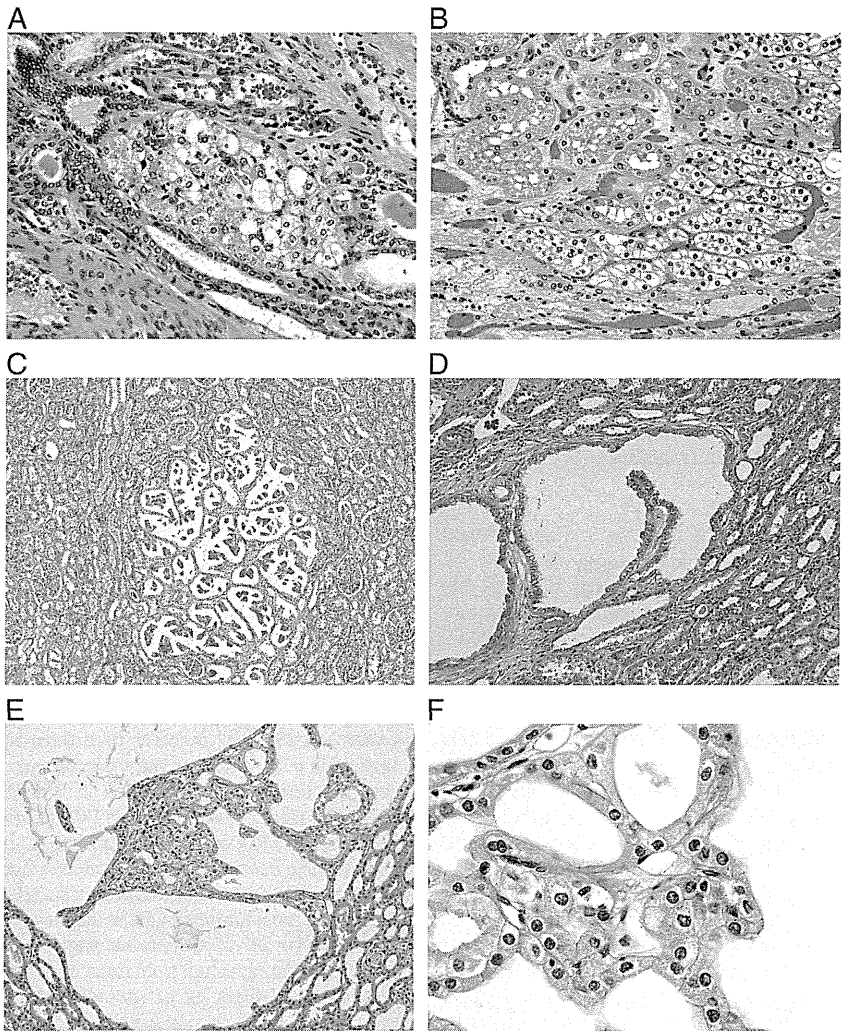

Fig. 4. Microscopic findings of renal parenchymal abnormalities of BHDS. (A), Renal parenchymal oncocytic change is seen. (B), Renal parenchyma with clear cell change can be noted. (C), Papillary adenoma is shown apart from the main tumor. (D), Small papillary tufts mimicking ITPSPT are observed in the grossly normally looking renal parenchyma. (E), Small chromophobe RCC-like lesion with cystic change and focal papillary architecture is seen at the renal parenchyma. (F), High magnification of (E). Shrunken nuclei, perinuclear halo, and distinct cell border are noted.

detailed clinical information. Renal oncocytosis without BHDS show no *FLCN* gene mutation [20,21]. The association of renal angiomyolipoma with BHDS has also been reported, and such findings may suggest the close relationship between BHDS and tuberous sclerosis [22]. The *FLCN* gene is located at chromosome 17p12q11 [15,19]. The exact mechanism how *FLCN* gene mutation is associated with renal tumor remains to be elucidated [22]. Probably, *FLCN* gene mutation may affect the progenitor cells of proximal tubules, distal tubules, or collecting ducts and cause various histologic subtypes as observed in the present study [12]. BHDS–associated renal tumors are genetically different from other renal neoplasia including chromophobe RCC and oncocytoma, and loss of *FLCN* expression is linked with increased mitochondrial gene expression [23]. These facts may explain why HOCT with deeply eosinophilic cytoplasm often occurs in BHDS. Although some investigators have reported that BHDS-associated renal tumors seldom recur or metastasize, other investigators have described metastatic or clinically aggressive cases [15,24]. Although we found that all patients were alive without recurrence and metastasis at the relative short period of follow-up in this study, it is imperative for pathologists to accurately diagnose BHDS-related renal tumors [25]. The multifocality does not affect outcome at an intermediate follow-up [26]. Regarding a management of renal tumors in this syndrome, bare observation of small tumors, until they reach 3 cm in size, is frequently recommended [2,24]. For therapeutic modality, nephron-sparing surgery has been attempted [24,27]. Patients with BHDS should be more aggressively managed than in non-BHDS because of its histologic discordance [16]. As FLCN protein negatively regulates the mammalian target of rapamycin pathway, mammalian target of rapamycin inhibitors may be effective in patients with metastatic disease [28].

Table 4
Immunohistochemical result of ITPSPT.

Case	CD82	CD10	RCC Marker	E-cadherin	CK7	CA9
1	d, +	−	−	d, +	d, +	NP
2	NP	NP	NP	NP	NP	NP
3	d, +	−	−	d, +	d, +	NP
4	NP	NP	NP	NP	NP	NP
5	d, +	−	−	d, +	d, +	−
6	d, +	NP	NP	NP	d, +	−

Abbreviations: *CK7*, cytokeratin 7; *d*, diffusely; *+*, positive; *−*, negative, *NP*, not performed.

Please cite this article as: Kuroda N, et al, Intratumoral peripheral small papillary tufts: a diagnostic clue of renal tumors associated with Birt-Hogg-Dubé syndrome, Ann Diagn Pathol (2014), http://dx.doi.org/10.1016/j.anndiagpath.2014.03.002

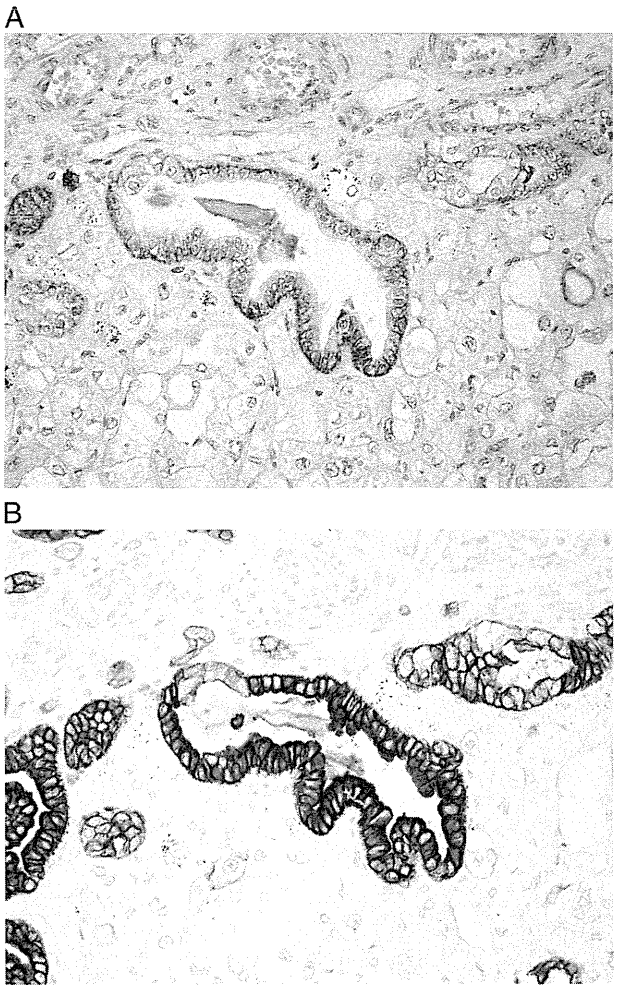

Fig. 5. Immunohistochemical results of ITPSPT. (A), ITPSPT are diffusely positive for CD82. (B), Cytokeratin 7 is diffusely expressed in ITPSPT.

Here, we found that ITPSPTs are frequent in the BHDS-associated renal tumors. This finding suggests that ITPSPT may be a precursor lesion of chromophobe RCC, HOCT, papillary adenoma, or papillary carcinoma because some ITPSPTs possessed perinuclear halo, binucleation, and prominent cell border in this study, and one case had papillary adenoma. This suggestion is supported by the positive reaction for CD82, cytokeratin 7, and E-cadherin, that is, markers frequently expressed in chromophobe RCC or papillary RCC [29,30]. Alternatively, ITPSPT may reflect entrapped cystic lesions, with reactive cytologic changes, often observed on the background renal parenchyma of BHDS [2,11,31]. We are not aware of description of papillary tufts or hyperplasia in the textbooks or in the previous reports. However, similar findings have been reported in patient who underwent long-term dialysis [32]. Therefore, it seems that ITPSPT may reflect an early neoplastic change. This suggestion is supported by the frequent association of a variety of histologic subtype of renal tumors in BHDS [4]. We suggest that ITPSPT and small chromophobe RCC-like lesion as shown in Fig. 3E and F may represent a sequential spectrum of the same lesion. Based on results of this study, the presence of ITPSPT seems to be more sensitive for the diagnosis of renal tumors linked with BHDS than multifocality or bilaterality. A large-scale study in the near future will be required to elucidate the pathologic significance of ITPSPT in BHDS-associated renal tumors.

In the present study, we found oncocytic and clear cell change of renal parenchyma. These lesions seem to be closely related to each other and may be precursor lesions of HOCT, chromophobe RCC, oncocytoma, clear cell RCC, or even hybrid chromophobe/clear cell RCC. In addition, small papillary tufts resembling ITPSPT in the normal-looking renal parenchyma were also observed in one case. Accordingly, we would like to emphasize the importance of identification of microscopic lesions including oncocytic change, clear cell change, small papillary tufts, and ITPSPTs in differential diagnosis of BHDS-associated renal tumors.

In conclusion, pathologists should keep in mind that combination of multifocality/bilaterality of renal tumors, the histologic discordance in multiple tumors, the presence of microscopic lesion such as oncocytic/clear cell change or papillary tufts/adenomas in renal parenchyma, and finding of ITPSPT as well as clinical information about skin lesions, pulmonary lesions, and family history may be vital clues in diagnosing renal tumors related to BHDS.

References

[1] Adley BP, Smith ND, Nayar R, Yang XJ. Birt-Hogg-Dubé syndrome. Clinicopathologic findings and genetic alterations. Arch Pathol Lab Med 2006;130:1865–70.
[2] Linehan WM, Pinto PA, Bratslavsky G, Pfaffenroth E, Merino M, Vocke CD, et al. Hereditary kidney cancer: unique opportunity for disease-based therapy. Cancer 2009;115:2252–61.
[3] Zbar B, Alvord G, Glenn G, Turner M, Pavlovich CP, Schmidt L, et al. Risk of renal and colonic neoplasms and spontaneous pneumothorax in the Birt-Hogg-Dubé syndrome. Cancer Epidermiol Biomarkers Prev 2002;11:393–400.
[4] Pavlovich CP, Walther MM, Eyler RA, Hewitt SM, Zbar B, Linehan WM, et al. Renal tumors in the Birt-Hogg-Dubé syndrome. Am J Surg Pathol 2002;26:1542–52.
[5] Schmidt LS. Birt-Hogg-Dubé syndrome, a genodermatosis that increases risk for renal carcinoma. Curr Mol Med 2004;4:877–85.
[6] Vocke CD, Yang Y, Pavlovich CP, Schmidt L, Nickerson ML, Torres-Cabala CA, et al. High frequency of somatic framesift BHD gene mutations in Birt-Hogg-Dubé-associated renal tumors. J Natl Cancer Inst 2005;97:931–5.
[7] Hansel DE. Genetic alterations and histopathologic findings in familial renal cell carcinoma. Histol Histopathol 2006;21:437–44.
[8] Abbosh PH, Grubb RL, Cao D, Humphrey PA. Hybrid renal tumors in Birt-Hogg-Dubé syndrome. J Urol 2011;186:2413–4.
[9] Houweling AC, Gijezen LM, Jonker MA, van Doorn MBA, Oldenburg RA, van Spaendonck-Zwarts KY, et al. Renal cancer and pneumothorax risk in Birt-Hogg-Dubé syndrome: an analysis of 115 *FLCN* mutation carriers from 35 BHD families. Br J Cancer 2011;105:1912–9.
[10] Nagashima Y, Furuya M, Gotohda H, Takagi S, Hes O, Michal M, et al. *FLCN* gene-mutated renal cell neoplasms: mother and daughter cases with a novel germline mutation. Int J Urol 2012;19:468–70.
[11] Furuya M, Tanaka R, Koga S, Yatabe Y, Gotoda H, Takagi S, et al. Pulmonary cyst of Birt-Hogg- Dubé syndrome: a clinicopathologic and immunohistochemical study of 9 families. Am J Surg Pathol 2012;36:589–600.
[12] Nickerson ML, Warren MB, Toro JR, Matrosova V, Glenn G, Turner ML, et al. Mutations in a novel gene lead to kidney tumors, lung wall defects, and benign tumors of the hair follicle in patients with the Birt-Hogg-Dubé syndrome. Cancer Cell 2002;2:157–64.
[13] Koga S, Furuya M, Takahashi Y, Tanaka R, Yamaguchi A, Yasufuku K, et al. Lung cysts in Birt-Hogg-Dubé syndrome: histopathological characteristics and aberrant sequence repeats. Pathol Int 2009;59:720–8.
[14] Palmirotta R, Savonarola A, Ludovici G, Donati P, Cavaliere D, DE Marchis ML, et al. Association between Birt Hogg Dubé syndrome and cancer predisposition. Anticancer Res 2010;30:751–8.
[15] Kluijt I, de Jong D, Teetstra HJ, Axwijk PH, Gille JJ, Bell K, et al. Early onset of renal cancer in a family with Birt-Hogg-Dubé syndrome. Clin Genet 2009;75:537–43.
[16] Boris R, Benhammou J, Merino M, Pinto PA, Linehan WM, Bratlavsky G. The impact of germline BHD mutation on histologic concordance and clinical management of patients with bilateral renal masses and known unilateral oncocytoma. J Urol 2011;185:2050–5.
[17] Khoo SK, Bradley M, Wong FK, Hedbald MA, Nordenskjöld M, Teh BT, et al. Birt-Hogg-Dubé syndrome: mapping of a novel hereditary neoplasia gene to chromosome 17p12-q11.2. Oncogene 2001;20:5239–42.
[18] Toro JR, Glenn G, Duray P, Darling T, Weirich G, Zbar B, et al. Birt-Hogg-Dubé syndrome. A novel marker of kidney neoplasia. Arch Dermatol 1999;135:1195–202.
[19] Schmidt LS, Warren MB, Nickerson ML, Weirich G, Matrosova V, Toro JR, et al. Birt-Hogg-Dubé syndrome, a genodermatosis associated with spontaneous pneumothorax and kidney neoplasia, maps to chromosome 17p11.2. Am J Hum Genet 2001;69:876–82.
[20] Kuroda N, Tanaka A, Ohe C, Mikami S, Nagashima Y, Sasaki T, et al. Review of renal oncocytosis (multiple oncocytic lesions) with focus on clinical and pathobiological aspects. Histol Histopathol 2012;27:1407–12.
[21] Nagashima Y, Mitsuya T, Shioi K, Noguchi S, Kishida T, Hamano A, et al. Renal oncocytosis. Pathol Int 2005;55:210–5.

Please cite this article as: Kuroda N, et al, Intratumoral peripheral small papillary tufts: a diagnostic clue of renal tumors associated with Birt-Hogg-Dubé syndrome, Ann Diagn Pathol (2014), http://dx.doi.org/10.1016/j.anndiagpath.2014.03.002